DISCRETE CONSTANT MEAN CURVATURE SURFACES AND THEIR INDEX

KONRAD POLTHIER AND WAYNE ROSSMAN

ABSTRACT. We define triangulated piece-wise linear constant mean curvature surfaces using a variational characterization, so that they are critical for area amongst continuous piece-wise linear variations which preserve the boundary and simplicial structure and also (in the nonminimal case) the volume to one side of the surface. We then find explicit examples, such as discrete minimal catenoids and helicoids.

We use these discretized surfaces to study the index of unstable minimal surfaces, by numerically evaluating the spectrum of their Jacobi operators, and this approach deviates from other numerical investigations in that we use a variational characterization to define the discrete approximating surfaces. Our numerical estimates confirm known results on the index of some smooth minimal surfaces, and provide additional information regarding their area-reducing variations.

1. INTRODUCTION

Smooth submanifolds, and surfaces in particular, with constant mean curvature (CMC) have a long history of study, and modern work in this field relies heavily on geometric and analytic machinery which has evolved over hundreds of years. However, nonsmooth surfaces are also natural mathematical objects, even though there is less machinery available for studying them. (Consider M. Gromov's approach of doing geometry using only a set with a measure and a measurable distance function [8].)

Here we consider piecewise-linear triangulated surfaces (we call them "discrete surfaces"), which have been brought more to the forefront of geometrical research by computer graphics. We define CMC for discrete surfaces in $\mathbb{R}^3$ so that they are critical for volume-preserving variations, just as smooth CMC surfaces are. Discrete CMC surfaces have both interesting differences from and similarities with smooth ones. For example, they are different in that smooth minimal graphs in $\mathbb{R}^3$ over a bounded domain are stable, whereas discrete minimal graphs can be highly unstable. We will explore properties like this in section 2.

And in section 3 we will see some ways in which these two types of surfaces are similar. We will see that: a discrete catenoid has an explicit description in terms of the hyperbolic cosine function, just as the smooth catenoid has; and a discrete helicoid can be described with the hyperbolic sine function, just as a conformally parametrized smooth helicoid is; and there are discrete Delaunay surfaces which have translational periodicities, just as smooth Delaunay surfaces have.

Pinkall and Polthier [16] used Dirichlet energy and a numerical minimization procedure to find discrete minimal surfaces. In this work, we rather have the goal to describe discrete minimal surfaces as explicitly as possible, and thus we are limited

to the more fundamental examples, for example the discrete minimal catenoid and helicoid. We note that these explicit descriptions will be useful for implementing a procedure that we describe in the next paragraphs.

Discrete surfaces have an advantage over smooth ones in the following way: Function spaces representing smooth variations of smooth surfaces are infinite dimensional, and hence the study of linear operators on these spaces is often very difficult. In particular, it is often difficult to get explicit information about the spectra of such operators. However, the function spaces of variations of discrete surfaces contain piece-wise linear functions and are finite dimensional, and linear operators then reduce to matrices. So the discrete case is much easier to handle.

This suggests that an useful procedure for studying the spectra of the linear Jacobi operator in the second variation formula of smooth CMC surfaces is to consider the corresponding spectra of discrete CMC approximating surfaces. (This is strongly related to the finite element method in numerical analysis; however, in our case the finite element approximations will have geometric and variational meaning in their own right.) As a particular example of this, consider that a problem of interest is to find the index (the number of negative points in the spectrum) of a smooth minimal surface, and that the standard approach to this problem is to replace the metric of the surface with the metric obtained by pulling back the spherical metric via the Gauss map. This approach can yield the index: for example, the index of a complete catenoid is 1 ([6]), the index of a complete Enneper surface is 1 ([6]), the index of a complete Jorge-Meeks n-noid is $2n - 3$ ([11], [10]) and the index of a complete genus k Costa-Hoffman-Meeks surface is $2k + 3$ for every $k \leq 37$ ([13], [12]). However, this approach does not yield the eigenvalues and eigenfunctions on compact portions of the original minimal surfaces, as the metric has been changed. It would be interesting to know the eigenfunctions associated to negative eigenvalues, since these represent the directions of variations that reduce area, and the above procedure can provide this information.

In sections 4 and 6 we establish some tools for studying the spectrum of discrete CMC surfaces, and then we test the above procedure on two simple cases – a (minimal) rectangle, and a portion of a smooth minimal catenoid bounded by two circles. In these two cases we know the spectra of the smooth surfaces (section 5), and we know approximating discrete CMC surfaces as well (section 3), so we can check that the above procedure produces good approximations for the eigenvalues and smooth eigenfunctions (section 7), which indeed must be the case, by the theory of the finite element method [3], [7]. With these successful tests, we go on to consider cases where we do not apriori know what the smooth eigenfunctions should be, such as the Jorge-Meeks 3-noid and the genus 1 Costa surface (section 7).

We note that the above procedure can also be implemented using discrete approximating surfaces which are found only numerically and not explicitly, such as surfaces found by the method in [16]. And in fact, we use the method in [16] to find approximating surfaces for the 3-noid and Enneper surface and Costa surface.

2. DISCRETE MINIMAL AND CMC SURFACES

We start with a variational characterization of discrete minimal and discrete CMC surfaces. This characterization will allow us to construct explicit *unstable* discrete CMC surfaces. (Note that merely finding minima for area with respect to a volume constraint would not suffice for this, as that would produce only stable examples.)
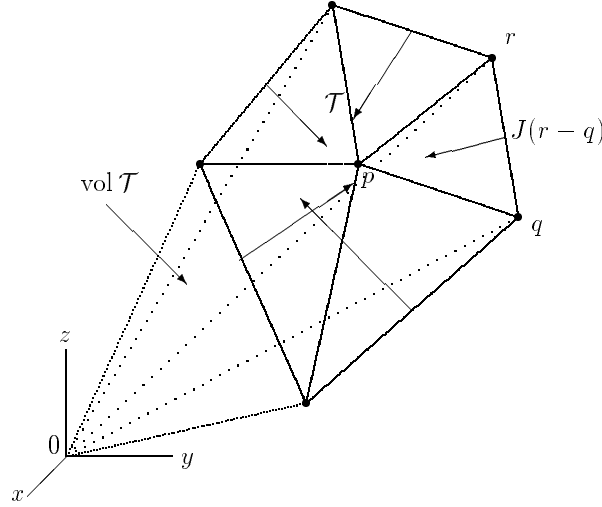
FIGURE 1

We will use CMC discrete surfaces that are unstable for our later numerical spectra computations.

The following definition for discrete surfaces works equally well for surfaces in $\mathbb{R}^n$, but, as our constructions will all be in $\mathbb{R}^3$, we restrict to this space.

Definition 2.1. *A discrete surface in $\mathbb{R}^3$ is a triangular mesh $\mathcal{T}$ which has the topology of an abstract 2-dimensional simplicial complex K combined with a geometric C^0-surface realization in $\mathbb{R}^3$. The geometric realization $|K|$ is determined by a set of vertices $\mathcal{V} = \{p_1, ..., p_n\} \subset \mathbb{R}^3$, and $\mathcal{T}$ can be identified with the pair $(K, \mathcal{V})$. The simplicial complex K represents the connectivity of the mesh. The 0, 1, and 2 dimensional simplices of K represent the vertices, edges, and triangles of the discrete surface.*

Let $T = (p, q, r)$ denote an oriented triangle of $\mathcal{T}$ with vertices $p, q, r \in \mathcal{V}$. Let $\overline{pq}$ denote an edge of T with endpoints $p, q \in V$.

For $p \in \mathcal{V}$, let $\mathrm{star}(p)$ denote the triangles of $\mathcal{T}$ that contain p as a vertex. For an edge $\overline{pq}$, let $\mathrm{star}(\overline{pq})$ denote the (at most two) triangles of $\mathcal{T}$ that contain $\overline{pq}$ as an edge.

The area of a discrete surface is

$$\mathrm{area}(\mathcal{T}) := \sum_{T \in \mathcal{T}} \mathrm{area}\, T \ ,$$

where $\mathrm{area}\, T$ denotes the area of the triangle T as a subset of $\mathbb{R}^3$.

Definition 2.2. *Let $\mathcal{V} = \{p_1, ..., p_n\}$ be the set of vertices of a discrete surface $\mathcal{T}$. A variation $\mathcal{T}(t)$ of $\mathcal{T}$ is defined as a C^2 variation of the vertices p_i*

$$p_i(t) : [0, \epsilon) \to \mathbb{R}^3 \ so \ that \ p_i(0) = p_i \ \forall i = 1, ..., n.$$

The straightness of the edges and the flatness of the triangles are preserved as the vertices move.

In the smooth situation, when the boundary is fixed, the variation space is typically restricted to normal variations, since the tangential parts of the variations only perform reparametrizations of the surfaces in the variations. However, on discrete surfaces there is an ambiguity in the choice of normal vectors at the vertices, so we allow arbitrary variations. But we will later see (section 7) that our experimental results can accurately estimate normal variations of a smooth surface when the discrete surface is a close approximation to the smooth surface.

In the following we derive the evolution equations for some basic entities under surface variations.

Let $\mathcal{T}(t)$ be a variation of a discrete surface $\mathcal{T}$. At each vertex p of $\mathcal{T}$, the gradient of area is

$$(1) \qquad \nabla_p \operatorname{area} \mathcal{T} = \frac{1}{2} \sum_{T=(p,q,r)\in \operatorname{star} p} J(r-q) \ ,$$

where J is rotation of angle $\frac{\pi}{2}$ in the plane of each oriented triangle T. The first derivative of the surface area is then given by the chain rule

$$\frac{d}{dt} \operatorname{area} \mathcal{T} = \sum_{p\in\mathcal{V}} \langle p', \nabla_p \operatorname{area} \mathcal{T} \rangle \ .$$

The volume of the surface is the oriented volume enclosed by the cone of the surface over the origin in $\mathbb{R}^3$

$$\operatorname{vol} \mathcal{T} := \frac{1}{6} \sum_{T=(p,q,r)\in\mathcal{T}} \langle p, q\times r \rangle = \frac{1}{3} \sum_{T=(p,q,r)\in\mathcal{T}} \langle \vec{N}, p \rangle \cdot \operatorname{area} T \ ,$$

where p is any of the three vertices of the triangle T and

$$\vec{N} = \frac{(q-p)\times(r-p)}{|(q-p)\times(r-p)|}$$

is the oriented normal of T. It follows that

$$(2)$$
$$\nabla_p \operatorname{vol} \mathcal{T} = \frac{1}{6} \sum_{T=(p,q,r)\in \operatorname{star} p} q\times r = \frac{1}{6} \sum_{T=(p,q,r)\in \operatorname{star} p} 2\cdot \operatorname{area} T \cdot \vec{N} + p\times(r-q)$$

and

$$\frac{d}{dt} \operatorname{vol} \mathcal{T} = \sum_{p\in\mathcal{V}} \langle p', \nabla_p \operatorname{vol} \mathcal{T} \rangle \ .$$

Note that if p is an interior vertex, then the boundary of $\operatorname{star} p$ is closed and $\sum_{T\in \operatorname{star} p} p\times(r-q) = 0$ disappears from $\nabla_p \operatorname{vol} \mathcal{T}$.

In the smooth case, a minimal surface is critical with respect to area for any variation that fixes the boundary, and a CMC surface is critical with respect to area for any variation that preserves volume and fixes the boundary. We wish to define discrete CMC surfaces so that they have the same variational properties for the same types of variations. So we will consider variations $\mathcal{T}(t)$ of $\mathcal{T}$ that fix the boundary $\partial\mathcal{T}$ and that additionally preserve volume in the nonminimal case, which we call *permissible variations*. The condition that makes a discrete surface area-critical for any permissible variation is expressed in the following definition.

Definition 2.3. *A discrete surface has* constant mean curvature *(*CMC*) if there exists a constant H so that ∇_p area $= H \nabla_p$ vol for all interior vertices p. If $H = 0$ then it is* minimal.

This definition for discrete minimality has been used in [16]. In contrast, our definition of discrete CMC surfaces differs from [14], where CMC surfaces are characterized algorithmically using discrete minimal surfaces in S^3 and a conjugation transformation. Compare also [2] for a definition via discrete integrable systems which lacks variational properties.

2.0.1. *Uniqueness of Discrete Minimal Disks.* Uniqueness of a bounded minimal surface with a given boundary ensures that it is stable, and uniqueness can sometimes be decided using the maximum principle of elliptic equations. For example, the maximum principle ensures that a minimal surface is contained in the convex hull of its boundary, and, if the boundary has a 1-1 projection to a convex planar curve, then it is unique for that boundary and is a minimal graph. The maximum principle also shows that any minimal graph is unique even when the projection of its boundary is not convex. More generally, stability still holds when the surface merely has a Gauss map image contained in a hemisphere, as shown in [1] (although their proof employs tools other than the maximum principle).

However, such statements do not hold for discrete minimal surfaces. Consider the surface shown in the left-hand side of Figure 2, whose height function has a local maximum at an interior vertex. This example does not lie in the convex hull of its boundary and thereby disproves existence of a discrete version of the maximum principle. Also, the three surfaces on the right-hand side in Figure 3 are all minimal graphs over a ring-like domain with the same boundary contours and simplicial structure, and yet they are not the same surfaces, hence graphs with given simplicial structure are not unique. And the left-hand surface in Figure 3 shows a surface whose Gauss map is contained in a hemisphere but which is unstable (this surface is not a graph) – another example of this property is the first ring-like surface in Figure 3, which is also unstable. (We define stability of discrete CMC surfaces in section 4).

The influence of the discretization on nonuniqueness, like as in the ring-like examples of Figure 3, can also be observed in a more trivial way for a discrete minimal graph over a simply connected convex domain. The two surfaces on the right-hand side of Figure 2 have the same trace, i.e. they are identical as geometric surfaces, but they are different as discrete surfaces. Interior vertices may be freely added and moved inside the middle planar square without affecting minimality.

In contrast to existence of these counterexamples we believe that some properties of smooth minimal surfaces remain true in the discrete setting, based on numerical experiments. We say that a discrete surface is a disk if it is homeomorphic to a simply connected domain.

Conjecture 2.1. *Let $\mathcal{T} \subset \mathbb{R}^3$ be a discrete minimal disk whose boundary projects injectively to a convex planar polygonal curve, then $\mathcal{T}$ is a graph over that plane.*

The authors were able to prove this conjecture with the extra assumption that all the triangles of the surface are acute, using the fact that the maximum principle (a height function cannot attain a strict interior maximum) actually does hold when all triangles are acute.
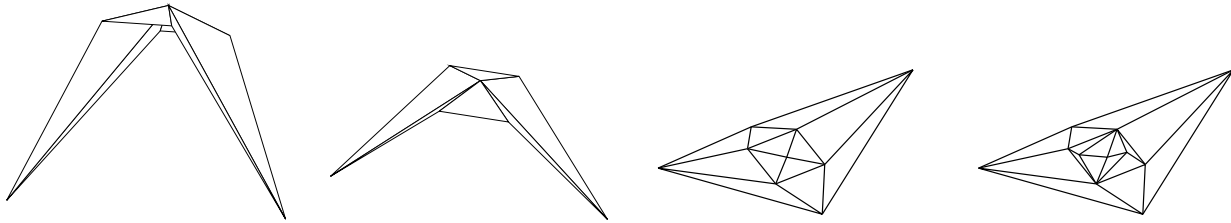
FIGURE 2. Two views on the left-hand side of a surface that de-
fies the maximum principle, and two discrete minimal surfaces on
the right-hand side with boundary vertices $(x, 0, z_1)$, $(-x, 0, z_1)$,
$(0, y, z_2)$, and $(0, -y, z_2)$ in $\mathbb{R}^3$. These two surfaces on the right
have the same trace in $\mathbb{R}^3$ but have different simplicial structures,
and a surprising feature of these examples is that the innermost
triangles form a square, regardless of the values of $x, y, z_1 \neq z_2$.

One can ask if a discrete minimal surface $\mathcal{T}$ with given simplicial structure and
boundary is unique if it has a 1-1 perpendicular or central projection to a convex
polygonal domain in a plane. The placement of the vertices need not be unique,
as we saw in the examples on the right-hand side of Figure 2, however, one can
consider if there is uniqueness in the sense that the trace of $\mathcal{T}$ in $\mathbb{R}^3$ is unique.

Conjecture 2.2. *Let $\Gamma \subset \mathbb{R}^3$ be a polygonal curve that either $\mathcal{A}$: projects injec-
tively to a convex planar polygonal curve, or $\mathcal{B}$: has a 1-1 central projection from
a point $p \in \mathbb{R}^3$ to a convex planar polygonal curve. Then, for each given simplicial
structure of disk type with boundary compatible to Γ, there exists a discrete minimal
disk $\mathcal{T}$ with boundary Γ and that simplicial structure, and the trace of $\mathcal{T}$ is uniquely
determined. Furthermore, $\mathcal{T}$ is a graph in the case $\mathcal{A}$, and $\mathcal{T}$ is contained in the
cone of Γ over p in the case $\mathcal{B}$.*

We have the following weaker form of Conjecture 2.2, which follows from Corol-
lary 4.1 of section 4 in the case that there is only one interior vertex:

Conjecture 2.3. *If a discrete minimal surface is a graph over a convex polygonal
domain, then it is stable.*

3. EXPLICIT DISCRETE SURFACES

Here we describe explicit discrete catenoids and helicoids, which seem to be the
first explicitly known nontrivial complete discrete minimal surfaces (with minimal-
ity defined variationally).

3.1. **Discrete Minimal Catenoids.** To derive an explicit formula for embedded
complete discrete minimal catenoids, we choose the vertices to lie on congruent
planar polygonal meridians, with the meridians placed so that the traces of the
surfaces will have dihedral symmetry. We will find that the vertices of a discrete
meridian lie equally spaced on a smooth hyperbolic cosine curve. Furthermore,
these discrete catenoids will converge uniformly in compact regions to the smooth
catenoid as the mesh is made finer.

We begin with a lemma that prepares the construction of the meridian of the
discrete minimal catenoid. We derive an explicit representation of the position of a
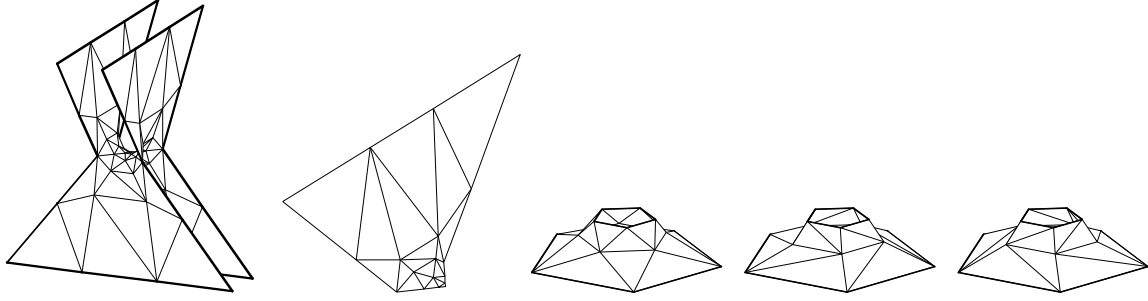
FIGURE 3. Two unstable and two stable discrete minimal surfaces
in $\mathbb{R}^3$. The first figure on the left is unstable, even though it is
locally a graph over a horizontal plane, in the sense that the third
coordinate of the normal vector to the surface is never zero. The
second figure on the left is one of the four congruent pieces of
the first figure. The middle figure (the leftmost annular graph)
is unstable, even though it is a graph over an annular polygonal
region in a horizontal plane, and it has area-reducing variations
that can deform to either of the last two stable minimal surfaces
on the right, which have the same simplicial structure.

vertex surrounded by four triangles in terms of the other four vertex positions. The
center vertex is assumed to be coplanar with each of the two pairs of two opposite
vertices, with those two planes becoming the plane of the vertical meridian and the
horizontal plane containing a dihedrally symmetric polygon (consisting of edges of
the surface).

Lemma 3.1. *Consider the vertex $p = (d, 0, e)$ surrounded by four vertices $q_1 = (a, 0, b)$, $q_2 = (d \cos \theta, d \sin \theta, e)$, $q_3 = (f, 0, g)$, and $q_4 = (d \cos \theta, -d \sin \theta, e)$, forming four triangles (p, q_1, q_2), (p, q_2, q_3), (p, q_3, q_4), and (p, q_4, q_1). Given real numbers a, b, d, e, and angle θ so that $b \neq e$, there exists a choice of real numbers f and g such that*

$$\nabla_p \operatorname{area}(\operatorname{star} p) = 0$$

if and only if

$$2ad > \frac{(e - b)^2}{1 + \cos \theta} \; .$$

Furthermore, when f and g exist, they are unique and must be of the form

$$
\begin{aligned}
f &= \frac{2(1 + \cos \theta)d^3 + (a + 2d)(e - b)^2}{2ad(1 + \cos \theta) - (e - b)^2} \; , \\
g &= 2e - b \; .
\end{aligned}
$$

Proof. First we note that the assumption $b \neq e$ is necessary. If $b = e$, then one may
choose $g = b$, and then there is a free 1-parameter family of choices of f.

For simplicity we apply a vertical translation and a homothety about the origin
of $\mathbb{R}^3$ to normalize $d = 1$, $e = 0$, and by doing a reflection if necesary, we may
assume $b < 0$. Let $c = \cos \theta$ and $s = \sin \theta$.

We derive conditions for the coordinate components of ∇_p area to vanish. The second component vanishes by symmetry of star p. Using the definitions

$$c_1 := \frac{(a-1)s^2 - b^2(1-c)}{\sqrt{2b^2(1-c) + (a-1)^2 s^2}} \,, \quad c_2 := \frac{ab+b}{\sqrt{2b^2(1-c) + (a-1)^2 s^2}} \,,$$

the first (resp. third) component of ∇_p area vanishes if

$$(3) \qquad c_1 = \frac{g^2(1-c) - (f-1)s^2}{\sqrt{2g^2(1-c) + (f-1)^2 s^2}} \,, \quad \text{resp.} \quad c_2 = \frac{-(f-1)g - 2g}{\sqrt{2g^2(1-c) + (f-1)^2 s^2}} \,.$$

Dividing one of these equations by the other we obtain

$$(4) \qquad\qquad\qquad f - 1 = \frac{c_2 g(1-c) + 2c_1}{c_2 s^2 - c_1 g} g \,,$$

so f is determined by g. It now remains to determine if one can find g so that $c_2 s^2 - c_1 g \neq 0$. If $f - 1$ is chosen as in equation 4, then the first minimality condition of equation 3 holds if and only if the second one holds as well. So we only need to insert this value for $f - 1$ into the first minimality condition and check for solutions g. When $c_1 \neq 0$, we find that the condition becomes

$$1 = \frac{c_2 s^2 - c_1 g}{|c_2 s^2 - c_1 g|} \frac{g}{|g|} \frac{-(1-c)g^2 - 2s^2}{\sqrt{2(1-c)c_2^2 s^4 + 4c_1^2 s^2 + (2(1-c)c_1^2 + s^2(1-c)^2 c_2^2)g^2}} \,.$$

Since $-(1-c)g^2 - 2s^2 < 0$, note that this equation can hold only if $c_2 s^2 - c_1 g$ and g have opposite signs, so the equation becomes

$$1 = \frac{(1-c)g^2 + 2s^2}{\sqrt{2(1-c)c_2^2 s^4 + 4c_1^2 s^2 + (2(1-c)c_1^2 + s^2(1-c)^2 c_2^2)g^2}} \,,$$

which simplifies to

$$1 = \frac{\sqrt{(1-c)g^2 + 2s^2}}{\sqrt{(1-c)c_2^2 s^2 + 2c_1^2}} \,.$$

This implies g^2 is uniquely determined. Inserting the value

$$g = \pm b \,,$$

one finds that the above equation holds. When $g = b < 0$, we find that $c_2 s^2 - c_1 g < 0$, which is impossible. When $g = -b > 0$, we find that $c_2 s^2 - c_1 g < 0$ if and only if $2a(1+c) > b^2$. And when $g = -b$ and $2a(1+c) > b^2$, we have the minimality condition when

$$f = \frac{2 + 2c + ab^2 + 2b^2}{2a + 2ac - b^2} \,.$$

Inverting the transformation we did at the beginning of this proof brings us back to the general case where d and e are not necessarily 1 and 0, and the equations for f and g become as stated in the lemma.

When $c_1 = 0$, we have $(a-1)(1+c) = b^2$ and $(f-1)(1+c) = g^2$, so, in particular, we have $a > 1$ and therefore $2a(1+c) > b^2$. The right-hand side of equation (3) implies $g = -b$ and $f = a$. Again, inverting the transformation from the beginning of this proof, we have that f and g must be of the form in the lemma for the case $c_1 = 0$ as well. $\square$
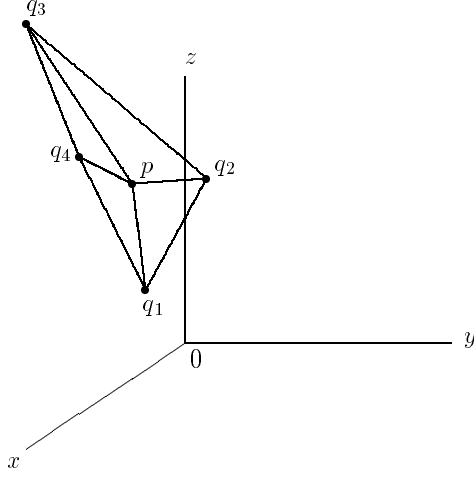
FIGURE 4. The construction in Lemma 3.1.

Note that the necessary and sufficient condition in the next lemma is identical to that of the previous lemma. This observation is crucial to the proof of the upcoming theorem.

Lemma 3.2. *Given two points (a, b) and (d, e) in $\mathbb{R}^2$ and an angle θ, with $b \neq e$, there exists an r so that these two points lie on some vertical translate of the curve*

$$\left(r \cosh \left[\frac{1}{e-b} \operatorname{arccosh} \left\{ 1 + \frac{1}{r^2} \frac{(e-b)^2}{1+\cos\theta} \right\} t \right], t \right) \quad , \quad t \in \mathbb{R} \, ,$$

if and only if $2ad > \frac{(e-b)^2}{1+\cos\theta}$.

Proof. Define $\hat{\delta} = \frac{e-b}{\sqrt{1+\cos\theta}}$. Without loss of generality, we may assume $0 < a \leq d$ and $e > 0$, and hence $-e \leq b < e$. If the points (a, b) and (d, e) both lie on the curve in the lemma, then

$$\operatorname{arccosh} \left(1 + \frac{\hat{\delta}^2}{r^2} \right) = \operatorname{arccosh} \left(\frac{d}{r} \right) - \operatorname{sign}(b) \cdot \operatorname{arccosh} \left(\frac{a}{r} \right) \, ,$$

where $\operatorname{sign}(b) = 1$ if $b \geq 0$ and $\operatorname{sign}(b) = -1$ if $b < 0$. Note that if $b = 0$, then a must equal r (and so $\operatorname{arccosh}(\frac{a}{r}) = 0$). This equation is solvable (for either value of $\operatorname{sign}(b)$) if and only if

$$\left(\frac{d}{r} + \sqrt{\frac{d^2}{r^2} - 1} \right) \left(\frac{a}{r} + \sqrt{\frac{a^2}{r^2} - 1} \right) = 1 + \frac{\hat{\delta}^2}{r^2} + \frac{\hat{\delta}}{r} \sqrt{2 + \frac{\hat{\delta}^2}{r^2}}$$

when $b \leq 0$, or

$$\frac{\frac{d}{r} + \sqrt{\frac{d^2}{r^2} - 1}}{\frac{a}{r} + \sqrt{\frac{a^2}{r^2} - 1}} = 1 + \frac{\hat{\delta}^2}{r^2} + \frac{\hat{\delta}}{r} \sqrt{2 + \frac{\hat{\delta}^2}{r^2}}$$

when $b \geq 0$, for some $r \in (0, a]$. The right-hand side of these two equations has the following properties:

1. It is a nonincreasing function of $r \in (0, a]$.
2. It attains some finite positive value at $r = a$.
3. It is greater than the function $2\hat{\delta}^2/r^2$.
4. It approaches $2\hat{\delta}^2/r^2$ asymptotically as $r \to 0$.

The left-hand sides of these two equations have the following properties:

1. They attain the same finite positive value at $r = a$.
2. The first one is a nonincreasing function of $r \in (0, a]$.
3. The second one is a nondecreasing function of $r \in (0, a]$.
4. The second one attains the value $\frac{d}{a}$ at $r = 0$.
5. The first one is less than the function $4ad/r^2$.
6. The first one approaches $4ad/r^2$ asymptotically as $r \to 0$.

So, from these properties it is clear that one of the two equations above has a solution for some r if and only if $2ad > \hat{\delta}^2$. This completes the proof. $\qquad\square$

We now derive an explicit formula for discrete minimal catenoids, which is given by specifying the vertices along planar polygonal meridians. Then the traces of the surfaces will have dihedral symmetry of order $k \geq 3$. The surfaces are tessellated by planar isosceles trapezoids like a $\mathbb{Z}^2$ grid, and each trapezoid can be triangulated into two triangles by choosing a diagonal of the trapeziod as the interior edge. Either diagonal can be chosen, as this does not affect the minimality of the catenoid.

The discrete catenoid has two surprising features. First, the vertices of a meridian lie on a smooth hyperbolic cosine curve (which is the profile curve of smooth catenoids), and there is no apriori reason to have expected this. Secondly, the vertical spacing of the vertices along the meridians is constant.

Theorem 3.1. *There exists a four-parameter family of embedded and complete discrete minimal catenoids $C = C(\theta, \delta, r, z_0)$ with dihedral rotational symmetry and planar meridians. If we assume that the dihedral symmetry axis is the z-axis, and a meridian lies in the xz-plane, then, up to vertical translation, the catenoid is completely described by the following properties:*

1. *$\theta = \frac{2\pi}{k}$, $k \in \mathbb{N}$, $k \geq 3$, is the dihedral angle.*
2. *The vertices of the meridian in the xz-plane interpolate the smooth $\cosh$ curve*

$$x(z) = r \cosh\left(\frac{1}{r}az\right),$$

   with

$$a = \frac{r}{\delta} \operatorname{arccosh}\left(1 + \frac{1}{r^2}\frac{\delta^2}{1 + \cos\theta}\right),$$

   where the parameter $r > 0$ is the waist radius of the interpolated $\cosh$ curve, and $\delta > 0$.
3. *For any given arbitrary initial value $z_0 \in \mathbb{R}$, the profile curve has vertices of the form*

$$\begin{aligned} z_j &= z_0 + j\delta \\ x_j &= x(z_j) \end{aligned}$$

   where δ is the constant vertical distance between adjacent vertices of the meridian.
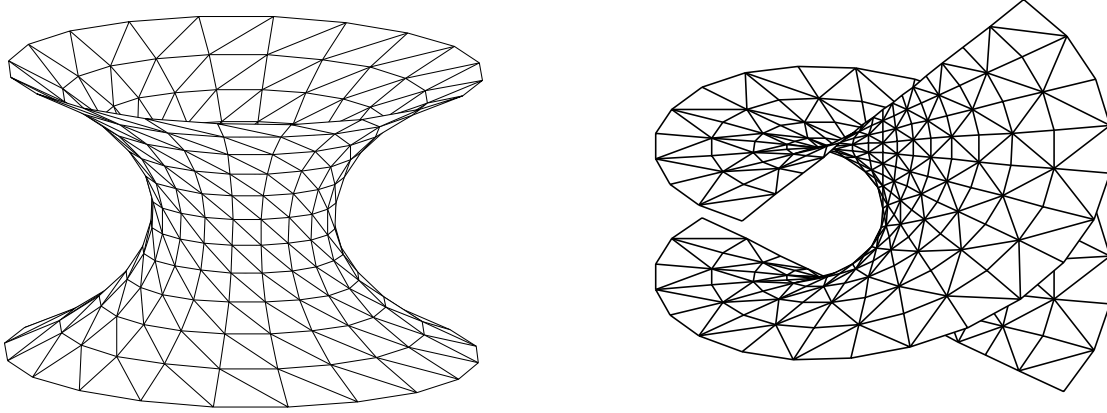
FIGURE 5. A discrete minimal catenoid and helicoid. (For this helicoid we have chosen $x_0 = 0$.)

4. *The planar trapezoids of the catenoid may be triangulated independently of each other.*

Proof. By Lemma 3.1, if we have three consequtive vertices $(x_{n-1}, z_{n-1}), (x_n, z_n)$, and (x_{n+1}, z_{n+1}) along the meridian (the profile curve in the xz-plane), they satisfy the recursion formula

$$(5) \qquad x_{n+1} = \frac{(x_{n-1} + 2x_n)\hat{\delta}^2 + 2x_n^3}{2x_n x_{n-1} - \hat{\delta}^2} \ , \quad z_{n+1} = z_n + \delta \ ,$$

where $\delta = z_n - z_{n-1}$ and $\hat{\delta} = \delta/\sqrt{1 + \cos\theta}$. As seen in Lemma 3.1, the vertical distance between (x_{n-1}, z_{n-1}) and (x_n, z_n) is the same as the vertical distance between (x_n, z_n) and (x_{n+1}, z_{n+1}), so we may consider δ and $\hat{\delta}$ to be constants independent of n.

In order for the surface to exist, Lemma 3.1 requires that

$$2x_n x_{n-1} > \hat{\delta}^2 \ .$$

This implies that all x_n have the same sign, and we may assume $x_n > 0$ for all n. Therefore the surface is embedded. Also, as the condition $2x_n x_{n-1} > \hat{\delta}^2$ implies

$$2x_{n+1}x_n = \frac{2x_n(x_{n-1} + 2x_n)\hat{\delta}^2 + 4x_n^4}{2x_n x_{n-1} - \hat{\delta}^2} > \frac{2x_n x_{n-1}\hat{\delta}^2}{2x_n x_{n-1} - \hat{\delta}^2} > \hat{\delta}^2 \ ,$$

we see, inductively, that x_j is defined for all $j \in \mathbb{Z}$. Hence the surface is complete.

One can easily check that the function $x(z)$ in the theorem also satisfies the recursion formula (5), in the sense that if $x_j := x(z_j)$, then these x_j satisfy this recursion formula. It only remains to note that, given two initial points (x_{n-1}, z_{n-1}) and (x_n, z_n) with $z_n > z_{n-1}$, there exists an r so that these two points lie on the curve $x(z)$ with our given δ and θ (up to vertical translation) if and only if $2x_n x_{n-1} > \hat{\delta}^2$, as shown in Lemma 3.2. $\square$

Remark 3.1. *If we consider the example where* $(x_1, z_1) = (1, 0)$ *and* $(x_2, z_2) = (1 + \hat{\delta}^2, \delta)$, *then the recursion formula implies that*

$$(x_n, z_n) = \left(1 + \sum_{j=1}^{n-1} 2^{j-1} a_{n-1,j} \hat{\delta}^{2j}, (n-1)\delta\right), \quad for \ n \geq 3,$$

where $a_{n-1,j}$ *is defined recursively by* $a_{n,m} = 0$ *if* $m < 0$ *or* $n < 0$ *or* $m > n$, $a_{0,0} = 1$, $a_{n,0} = 2$ *if* $n > 0$, *and* $a_{n,m} = 2a_{n-1,m} - a_{n-2,m} + a_{n-1,m-1}$ *if* $n \geq m \geq 1$. *Thus*

$$a_{n,m} = \left(\begin{array}{c} n+m \\ 2m \end{array} \right) + \left(\begin{array}{c} n+m-1 \\ 2m \end{array} \right).$$

These $a_{n,m}$ *are closely related to the recently solved refined alternating sign matrix conjecture* [4].

Corollary 3.1. *There exists a two-parameter family of discrete catenoids* $C_1(\theta, z_0)$ *whose vertices interpolate the smooth minimal catenoid with meridian* $x = \cosh z$.

Proof. The waist radius of the discrete meridian must be $r = 1$. Further, we must choose the parameter $a = 1$ which is fulfilled if θ and δ are related by $1 + \cos\theta + \delta^2 = (1 + \cos\theta)\cosh\delta$. The offset parameter z_0 may be chosen arbitrarily leading to a vertical shift of the vertices along the smooth catenoid. $\square$

Corollary 3.2. *For each fixed* r *and* z_0, *the profile curves of the discrete catenoids* $C(\theta, \delta, r, z_0)$ *approach the profile curve* $x = r \cosh\frac{z}{r}$ *of a smooth catenoid uniformly in compact sets of* $\mathbb{R}^3$ *as* $\delta, \theta \to 0$.

Proof. Since

$$\lim_{\delta \to 0} \frac{1}{\delta} \operatorname{arccosh}(1 + \frac{1}{r^2} \frac{\delta^2}{1 + \cos\theta}) = \frac{\sqrt{2}}{r\sqrt{1 + \cos\theta}},$$

it follows that the profile curve of the discrete catenoid converges uniformly (in C^0 sense) to the curve

$$x = r \cosh\frac{\sqrt{2}z}{r\sqrt{1 + \cos\theta}}$$

as $\delta \to 0$. Then, as $\theta \to 0$ we approach the profile curve $x = r \cosh\frac{z}{r}$. $\square$

3.2. **Discrete Minimal Helicoids.** We continue on to the derivation of explicit discrete helicoids, which are a natural second example of complete, embedded discrete minimal surfaces.

In the smooth setting, there exists an isometric deformation through conjugate surfaces from the catenoid to the helicoid (see, for example, [15]). So, one might first try to make a similar deformation from the discrete catenoids in Theorem 3.1 to discrete minimal helicoids. But such a deformation appears to be impossible – in fact, in order to make an associate family of discrete minimal surfaces, one must allow non-continuous triangle nets having greater flexibility, as described in [17].

Therefore, we adopt a different approach for finding discrete minimal helicoids. The helicoids will be comprised of planar quadrilaterals, each triangulated by four coplanar triangles, see Figure 5. Each quadrilateral is the star of a unique vertex, and none of its four boundary edges are vertical or horizontal, and one pair of opposite vertices in its boundary have the same z-coordinate, and the four boundary
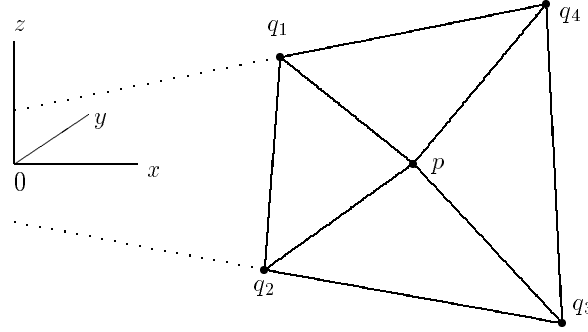
FIGURE 6. The construction in Lemma 3.3.

edges consist of two adjacent pairs of edges of equal length. First we derive an explicit representation of the center vertex of a typical vertex star of the helicoid:

Lemma 3.3. *Let p be a point with a vertex star consisting of four vertices q_1, q_2, q_3, q_4 and four triangles $\triangle_i = (p, q_i, q_{i+1})$, $i \in \{1, 2, 3, 4\}$ (mod 4). We assume that $p = (u, 0, 0)$, $q_1 = (b \cos \theta, b \sin \theta, 1)$, $q_2 = (b \cos \theta, -b \sin \theta, -1)$, $q_3 = (t \cos \theta, -t \sin \theta, -1)$, $q_4 = (t \cos \theta, t \sin \theta, 1)$ with real numbers $b < u < t$ and $\theta \in (0, \frac{\pi}{2})$.*
If either

$$t = -b(1 + 2u^2 \sin^2 \theta) + 2u \sqrt{1 + b^2 \sin^2 \theta} \sqrt{1 + u^2 \sin^2 \theta} \quad \text{or}$$

$$b = -t(1 + 2u^2 \sin^2 \theta) + 2u \sqrt{1 + t^2 \sin^2 \theta} \sqrt{1 + u^2 \sin^2 \theta} \,,$$

then ∇_p area vanishes.

Proof. Consider the conormals $J_1 = J(q_2 - q_1)$, $J_2 = J(q_3 - q_2)$, $J_3 = J(q_4 - q_3)$, $J_4 = J(q_1 - q_4)$, where J denotes oriented rotation by angle $\frac{\pi}{2}$ in the triangle $\triangle_j$ containing the edge being rotated. Then

$$J_1 = (2 \sqrt{1 + b^2 \sin^2 \theta}, 0, 0) \quad \text{and} \quad J_3 = (-2 \sqrt{1 + t^2 \sin^2 \theta}, 0, 0) \,.$$

Since $\langle J_4, (\cos \theta, \sin \theta, 0) \rangle = 0$ and $\det(J_4, (\cos \theta, \sin \theta, 0), (u - b \cos \theta, -b \sin \theta, -1)) = 0$ and $|J_4|^2 = (t - b)^2$, we have that the first component of J_4 (and also of J_2) is

$$\frac{u(t - b) \sin^2 \theta}{\sqrt{1 + u^2 \sin^2 \theta}} \,.$$

By symmetry, the second and third components of J_2 and J_4 are equal but opposite in sign, hence the second and third components of $J_1 + J_2 + J_3 + J_4$ are zero. So for the minimality condition to hold at p, we need that the first component of $J_1 + J_2 + J_3 + J_4$ is also zero, that is, we need

$$\frac{u(t - b) \sin^2 \theta}{\sqrt{1 + u^2 \sin^2 \theta}} + \sqrt{1 + b^2 \sin^2 \theta} - \sqrt{1 + t^2 \sin^2 \theta} = 0 \,,$$

and the solution of this with respect to b or t is as in the lemma. So, for this solution, ∇_p area vanishes. $\qquad\square$

FIGURE 7. Discrete analogues of cylinders and Delaunay surfaces.

Theorem 3.2. *There exists a family of complete embedded discrete minimal helicoids, with the connectivity as shown in Figure 5. The vertices, indexed by $i, j \in \mathbb{Z}$, are the points*

$$\frac{r \sinh(x_0 + j\delta)}{\sin \theta}(\cos(i\theta), \sin(i\theta), 0) + (0, 0, ir) \ ,$$

for any given reals $\theta \in (0, \frac{\pi}{2})$ and $r, \delta \in \mathbb{R}$.

Note that these surfaces are invariant under the screw motion that combines vertical upward translation of distance $2r$ with rotation about the x_3-axis by an angle of 2θ. The term x_0 determines the offset of the vertices from the z-axis, and δ determines the horizontal spacing of the vertices. The homothety factor is r, which equals the vertical distance between consecutive horizontal lines of edges.

Proof. Without loss of generality, we may assume $r = 1$. So for a given i, the vertices are points on the line $\{s(\cos(i\theta), \sin(i\theta), i) \,|\, s \in \mathbb{R}\}$, for certain values of s. We choose x_0 and δ so that the $(j-2)$'th vertex has s-value $s_{j-2} = \sinh(x_0 + (j-2)\delta)/\sin \theta$ and the $(j-1)$'th vertex has s-value $s_{j-1} = \sinh(x_0 + (j-1)\delta)/\sin \theta$. Lemma 3.3 implies that the j'th vertex has s-value

$$s_j = -s_{j-2}(1 + 2s_{j-1}^2 \sin^2 \theta) + 2s_{j-1}\sqrt{1 + s_{j-2}^2 \sin^2 \theta}\sqrt{1 + s_{j-1}^2 \sin^2 \theta} \ ,$$

a recursion formula that is satisfied by

$$s_j = \sinh(x_0 + j\delta)/\sin \theta \ .$$

Lemma 3.3 implies a similar formula for determining s_{j-3} in terms of s_{j-2} and s_{j-1}, with the same solution. Finally, noting that those vertices whose star is a planar quadrilateral can be freely moved inside that planar quadrilateral without disturbing minimality of the surface, the theorem is proved. $\square$

3.3. Discrete Cylinders and Delaunay Surfaces.

We now describe some ways one can find discrete analogues of cylinders and Delaunay surfaces. The simplest way is to choose positive reals a and e and an integer $k \geq 3$, and then choose the vertices to be

$$p_{j,\ell} = (a\cos(2\pi j/k), a\sin(2\pi j/k), e\ell)$$

for $j, \ell \in \mathbb{Z}$. We then make a grid of rectangular faces, and cut the faces by diagonals with endpoints $p_{j,\ell}$ and $p_{j+1,\ell+1}$. This is a discrete CMC surface with $H = a^{-1}(\cos(\pi/k))^{-1}$. It is interesting to note that H is independent of the value of e. See the left-hand side of Figure 7.

Another example is to choose positive reals a, b, e, and an integer $k \geq 3$, and to choose the vertices to be

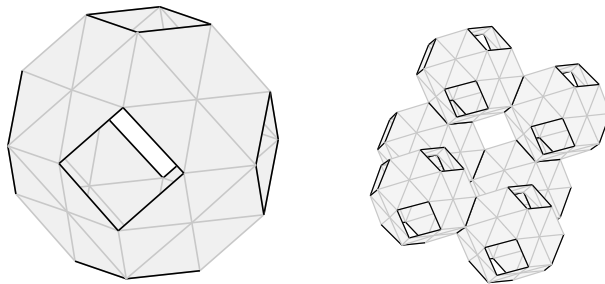$$p_{j,\ell} = (a\cos(2\pi j/k), a\sin(2\pi j/k), e\ell) \text{ when } j + \ell \text{ is even, and}$$

FIGURE 8. A triply-periodic discrete minimal surface, whose stability properties have been investigated by Karsten Groβe Brauckmann. On the left is a fundamental piece, and such pieces are attached as on the right to make an infinite-topology surface with the same symmetry as the $\mathbb{Z}^3$ cubic lattice in $\mathbb{R}^3$.

$$p_{j,\ell} = (b\cos(2\pi j/k), b\sin(2\pi j/k), e\ell) \text{ when } j + \ell \text{ is odd,}$$

for $j, \ell \in \mathbb{Z}$. We then make a grid of quadrilateral faces, and cut the faces by diagonals with endpoints $p_{j,\ell}$ and $p_{j+1,\ell+1}$ if $j + \ell$ is even, and by diagonals with endpoints $p_{j,\ell+1}$ and $p_{j+1,\ell}$ if $j + \ell$ is odd. By symmetry, it is clear that $\nabla_{p_{j,\ell}} area$ and $\nabla_{p_{j,\ell}} vol$ are parallel at each vertex; and for each value of e, one can then show the existence of values of a and b so that H is the same value at all vertices, using an intermediate value argument. Thus a discrete CMC cylinder is produced. See the second surface in Figure 7.

A third example can be produced by taking the vertices to be

$$p_{j,\ell} = (a\cos(2\pi j/k), a\sin(2\pi j/k), e\ell) \text{ when } \ell \text{ is even, and}$$

$$p_{j,\ell} = (b\cos(2\pi j/k), b\sin(2\pi j/k), e\ell) \text{ when } \ell \text{ is odd,}$$

for $j, \ell \in \mathbb{Z}$. We then make a grid of isosceles trapezoidal faces, and put an extra vertex in each of the trapezoidal faces, and connect this extra vertex by edges to each of the four vertices of the surrounding trapezoid. Keeping the placement of the vertices of the surface as symmetric as possible, one must move these extra vertices in $\mathbb{R}^3$ so that $\nabla area$ and ∇vol become parallel at these vertices, and then one must solve so that H has the same value at all vertices of the surface. This can be done numerically. See the last two examples in Figure 7.

Remark 3.2. *The 2-dimensional boundaries of the tetrahedron, octahedron, and icosahedron are discrete CMC surfaces. The boundaries of the cube and dodecahedron are not discrete surfaces in our sense, as they are not triangulated. However, by adding a vertex to the center of each face and connecting it by edges to each vertex in the boundary of the face, we can make discrete surfaces, and then we can move these face-centered vertices perpendicularly to the faces to adjust the mean curvature.*

4. SECOND VARIATION OF AREA

We now begin to consider the spectra of the second variation for discrete CMC surfaces, which necessarily starts with a technical and explicit computation of the second variation. For notating area and volume, we shall now frequently use "a"

and "V" instead of "area" and "vol", for brevity. We will also use $|T|$ or $|(p,q,r)|$ to signify the area of a triangle $T = (p,q,r)$.

Lemma 4.1. *For a compact discrete* CMC H *surface* $\mathcal{T}$ *with vertex set* $\mathcal{V}$,

$$a''(0) := \frac{\partial^2}{\partial^2 t} \text{area}(\mathcal{T})\bigg|_{t=0} = \sum_{p \in \mathcal{V}} \langle p', (\nabla_p a)' - H(\nabla_p V)' \rangle$$

for any permissible variation.

Proof.

$$a''(0) = \sum_{p \in \mathcal{V}} \langle p'', \nabla_p a \rangle + \langle p', (\nabla_p a)' \rangle = \sum_{p \in \mathcal{V}} \langle p'', H\nabla_p V \rangle + \sum_{p \in \mathcal{V}} \langle p', (\nabla_p a)' \rangle.$$

For a minimal discrete surface, the first term on the right hand side is clearly 0. For a discrete CMC surface with $H \neq 0$, the variation $p(t)$ is volume preserving, so

$$\frac{\partial \text{vol}(\mathcal{T})}{\partial t} = 0 \; \forall t \Longrightarrow \sum_p \langle p', \nabla_p V \rangle = 0 \; \forall t \Longrightarrow \sum_p \langle p'', \nabla_p V \rangle + \langle p', (\nabla_p V)' \rangle = 0 \,,$$

proving the lemma. $\qquad\square$

Definition 4.1. *A minimal or* CMC *discrete surface* $\mathcal{T}$ *is stable if $a''(0) \geq 0$ for any permissible variation.*

We now consider a vector-valued function $v_{p_j} \in \mathbb{R}^3$ that is defined on the n interior vertices $\mathcal{V}_{int} = \{p_1, ..., p_n\}$ of $\mathcal{T}$. We may extend this function to the boundary vertices of $\mathcal{T}$ as well, by assuming $v_p = \vec{0} \in \mathbb{R}^3$ for each boundary vertex p. The vectors v_{p_j} are the variation vector field of any boundary-fixing variation of the form

$$p_j(t) = p_j + t \cdot v_{p_j} + \mathcal{O}(t^2).$$

The fact that we have already restricted to boundary-fixing variations is no obstruction, as we will always consider only permissible variations. We define the vector $\vec{v} \in \mathbb{R}^{3n}$ by

$$\vec{v}^t = (v_{p_1}^t, ..., v_{p_n}^t).$$

We will now find a symmetric $3n \times 3n$ matrix Q (also considered as a bilinear form), so that $\vec{v}^t Q \vec{v}$ is equal to $a''(0)$ for any permissible variation with variation vector field $\vec{v}$. We define

$$\tau(\vec{v}) := \sum_{p \in \mathcal{V}} \langle v_p, (\nabla_p a)' \rangle = \sum_{p \in \mathcal{V}} \langle v_p, \frac{1}{2} \sum_{T=(p,q,r) \in \text{star}(p)} \vec{N} \times (r' - q') + \vec{N}' \times (r - q) \rangle$$

and

$$\mu(\vec{v}) := \sum_{p \in \mathcal{V}} \langle v_p, (\nabla_p V)' \rangle,$$

and so $a''(0) = \tau(\vec{v}) - H\mu(\vec{v})$ for any permissible variation with variation vector field $\vec{v}$. The purpose of the next two propositions is to find matrices Q_a and Q_V so that $\tau(\vec{v}) = \vec{v}^t Q_a \vec{v}$ and $\mu(\vec{v}) = \vec{v}^t Q_V \vec{v}$. Thus $Q = Q_a - HQ_V$.

Proposition 4.1. *There is a symmetric bilinear form represented by a $3n \times 3n$ matrix Q_a, where Q_a can be considered as an $n \times n$ grid with a 3×3 entry $Q_{a,p_i p_j}$ for each pair of interior vertices $p_i, p_j \in \mathcal{V}_{int}$ of $\mathcal{T}$, so that*

$$\tau(\vec{v}) = \vec{v}^{\,t} Q_a \vec{v}$$

for the variation vector field $\vec{v}$ of any permissible variation. The entry $Q_{a,p_i p_j}$ is 0 if the vertices p_i, p_j are not adjacent, and is

$$Q_{a,p_i p_j} = \frac{1}{2} \sum_{(p_i,p_j,r) \in star(\overline{p_i p_j})} \frac{1}{|p_i - p_j|^2} \big((p_i - p_j) \cdot J^t (p_i - p_j)$$

$$-J(p_i - p_j) \cdot (p_i - p_j)^t\big) - \cot \theta_{(p_i,p_j,r)} \vec{N}_{(p_i,p_j,r)} \cdot \vec{N}^{\,t}_{(p_i,p_j,r)}$$

for p_i and p_j adjacent and unequal, where $\theta_{(p_i,p_j,r)}$ is the interior angle of the triangle (p_i, p_j, r) at r, and is

$$Q_{a,p_i p_i} = \frac{1}{4} \sum_{(p_i,q,r) \in \mathrm{star}(p_i)} \frac{|r - q|^2}{|(p_i,q,r)|} \vec{N}_{(p_i,q,r)} \vec{N}^{\,t}_{(p_i,q,r)}$$

when the vertices are both equal to p_i. Here, $\vec{N}_{(p,q,r)}$ denotes the oriented unit normal vector of the triangle (p, q, r) (which we will subsequently abbreviate to $\vec{N}$).

Proof. If $\vec{v}$ and $\vec{w}$ are variation vector fields for any pair of permissible variations, we can define a bilinear form

$$Q_a(\vec{v}, \vec{w}) := \frac{1}{2} \sum_{T=(p,q,r) \in \mathcal{T}}$$

$$-\langle v_p \times w_r - v_r \times w_p + v_q \times w_p - v_p \times w_q + v_r \times w_q - v_q \times w_r, \vec{N}\rangle +$$

$$\frac{1}{2|T|} \langle v_p \times (r - q) + v_q \times (p - r) + v_r \times (q - p),$$

$$w_p \times (r - q) + w_q \times (p - r) + w_r \times (q - p)\rangle -$$

$$\frac{1}{2|T|} \langle v_p \times (r - q) + v_q \times (p - r) + v_r \times (q - p), \vec{N}\rangle \cdot$$

$$\langle w_p \times (r - q) + w_q \times (p - r) + w_r \times (q - p), \vec{N}\rangle .$$

Using $\vec{N}' = \frac{(q-p) \times (r'-p') + (q'-p') \times (r-p)}{2|T|} - \frac{\vec{N}}{2|T|} \langle (q-p) \times (r'-p') + (q'-p') \times (r-p), \vec{N}\rangle$, it follows that $\tau(\vec{v}) = Q_a(\vec{v}, \vec{v})$. Q_a is clearly bilinear, and the last two terms of Q_a are obviously symmetric in $\vec{v}$ and $\vec{w}$. The first term is also symmetric in $\vec{v}$ and $\vec{w}$, since $v_p \times w_r - v_r \times w_p = w_p \times v_r - w_r \times v_p$, $v_q \times w_p - v_p \times w_q = w_q \times v_p - w_p \times v_q$, and $v_r \times w_q - v_q \times w_r = w_r \times v_q - w_q \times v_r$.

It only remains to determine an explicit form for Q_a. For a given interior vertex p, suppose $\vec{v}$ and $\vec{w}$ are nonzero only at p, that is, that $\vec{v}^{\,t} = (0^t, ..., 0^t, v_p^t, 0^t, ..., 0^t)$ and $\vec{w}^{\,t} = (0^t, ..., 0^t, w_p^t, 0^t, ..., 0^t)$. Then

$$Q_a(\vec{v}, \vec{w}) = Q_{a,pp}(v_p, w_p) = \frac{1}{4} \sum_{T=(p,q,r) \in \mathrm{star}(p)}$$

$$\frac{1}{|T|}\langle v_p \times (r-q), w_p \times (r-q)\rangle - \frac{1}{|T|}\langle v_p \times (r-q), \vec{N}\rangle\langle w_p \times (r-q), \vec{N}\rangle$$

$$= \frac{1}{4} \sum_{T=(p,q,r)\in\mathrm{star}(p)}$$

$$\frac{1}{|T|}v_p^t(|r-q|^2 I - (r-q)(r-q)^t - ((r-q)\times\vec{N})((r-q)\times\vec{N})^t)w_p$$

$$= \frac{1}{4} \sum_{T=(p,q,r)\in\mathrm{star}(p)} \frac{|r-q|^2}{|T|}v_p^t(\vec{N}\vec{N}^t)w_p \;,$$

hence $Q_{a,pp}$ is of the form in the proposition.

Now suppose $\vec{v}^t = (0^t,...,0^t,v_p^t,0^t,...,0^t)$ and $\vec{w}^t = (0^t,...,0^t,w_q^t,0^t,...,0^t)$ for some given unequal interior vertices p and q. If p and q are not connected by some edge of the surface, then clearly $Q_a(\vec{v},\vec{w}) = 0$, so assume that p and q are adjacent. Note that $\mathrm{star}(\overline{pq})$ then contains two triangles (p,q,r_j) for $j=1,2$ and precisely one of them is properly oriented. Noting also that the normal vector $\vec{N}$ of a triangle changes sign when the orientation of the triangle is reversed, we have the following equation:

$$Q_a(\vec{v},\vec{w}) = Q_{a,pq}(v_p,w_q) = \frac{1}{2} \sum_{T=(p,q,r_k),k=1,2} \langle v_p \times w_q, \vec{N}\rangle +$$

$$\frac{1}{2|T|}\langle v_p \times (r_k-q), w_q \times (p-r_k)\rangle - \frac{1}{2|T|}\langle v_p \times (r_k-q), \vec{N}\rangle\langle w_q \times (p-r_k), \vec{N}\rangle =$$

$$= \frac{1}{4} \sum_{k=1}^{2} \frac{1}{|T|} v_p^t\left((p-r_k)(q-r_k)^t - (q-r_k)(p-r_k)^t - \langle p-r_k, q-r_k\rangle\vec{N}\vec{N}^t\right) w_q \;.$$

For a triangle (p,q,r), one can check that

$$(p-r)(q-r)^t - (q-r)(p-r)^t =$$

$$\frac{2|(p,q,r)|}{|p-q|^2}\left((p-q)(J(p-q))^t - J(p-q)(p-q)^t\right) \;,$$

so $Q_{a,pq}$ is as in the proposition. $\square$

Proposition 4.2. *There is a symmetric bilinear form represented by a $3n \times 3n$ matrix Q_V, where Q_V has a 3×3 entry Q_{V,p_ip_j} for each pair of vertices $p_i, p_j \in \mathcal{V}_{int}$ of $\mathcal{T}$, so that*

$$\mu(\vec{v}) = \vec{v}^t Q_V \vec{v}$$

for the variation vector field $\vec{v}$ of any permissible variation. We have $Q_{V,p_ip_i} = 0$, and $Q_{V,p_ip_j} = 0$ when the vertices p_i and p_j are not adjacent, and

$$Q_{V,p_ip_j} = \frac{1}{6}\begin{pmatrix} 0 & r_{2,3}-r_{1,3} & r_{1,2}-r_{2,2} \\ r_{1,3}-r_{2,3} & 0 & r_{2,1}-r_{1,1} \\ r_{2,2}-r_{1,2} & r_{1,1}-r_{2,1} & 0 \end{pmatrix}$$

for adjacent unequal p_i and p_j, where (p_i,p_j,r_k) are the two triangles in $\mathrm{star}(\overline{p_ip_j})$ and $r_k = (r_{k,1},r_{k,2},r_{k,3})$ for $k=1,2$, and (p_i,p_j,r_2) is properly oriented and (p_i,p_j,r_1) is not.

Proof.

$$\sum_{p \in \mathcal{V}} \langle p', (\nabla_p V)' \rangle = \sum_{p \in \mathcal{V}_{int}} \langle v_p, \frac{1}{6} \sum_{(p,q,r) \in \mathrm{star}(p)} (q \times r)' \rangle$$

$$= \frac{1}{6} \sum_{p \in \mathcal{V}_{int}} \left(\sum_{q \text{ adjacent to } p, q \neq p} \langle v_p \times v_q, r_2 - r_1 \rangle \right),$$

where (p, q, r_2) is the properly oriented triangle in $\mathrm{star}(\overline{pq})$, and (p, q, r_1) is the non-properly oriented triangle in $\mathrm{star}(\overline{pq})$. Thus we have

$$\mu(\vec{v}) = \sum_{p \in \mathcal{V}_{int}} \left(\sum_{q \text{ adjacent to } p, q \neq p} v_p^t (Q_{V,pq}) v_q \right),$$

where $Q_{V,pq}$ is a 3×3 matrix defined as in the proposition. Thus $Q_{V,pp} = 0$, and the fact that $Q_{V,pq}$ is skew-symmetric in p and q implies Q_V is symmetric. $\qquad\square$

Corollary 4.1. *If a discrete* CMC *surface* $\mathcal{T}$ *has only one interior vertex, then it is stable.*

Proof. Denote the single interior vertex by p, so $\mathrm{star}(p) = \mathcal{T}$. Then $Q_a = Q_{a,pp}$ and $Q_V = Q_{V,pp}$ are 3×3 matrices. By Propositions 4.1 and 4.2, $Q_V = 0$ and for any vector $u_p \in \mathbb{R}^3$ at p we have

$$u_p^t Q_a u_p = \frac{1}{4} \sum_{(p,q,r) \in \mathcal{T}} \frac{|r - q|^2}{|(p,q,r)|} u_p^t \vec{N} \vec{N}^t u_p = \frac{1}{4} \sum_{(p,q,r) \in \mathcal{T}} \frac{|r - q|^2}{|(p,q,r)|} \langle u_p, \vec{N} \rangle^2 \geq 0,$$

so $a''(0) \geq 0$ for all permissible variations. $\qquad\square$

5. Jacobi Operator for Smooth CMC Surfaces

We now are able to begin the study of the spectra of the second variation of discrete CMC surfaces, as the second variation is now in an explicit form. However, we postpone this to the next section, in order to discuss the spectra of the second variation of smooth CMC surfaces here. We digress to the smooth case for later comparison with the discrete case (section 7). In particular, here we explicitly determine the eigenvalues and eigenfunctions of the Jacobi operator for portions of smooth catenoids.

Let $\Phi : M \to \mathbb{R}^3$ be an immersion of a compact 2-dimensional surface M. Let $\vec{N}$ be a unit normal vector field on $\Phi(M)$ (we write $\Phi^* \vec{N}$ simply as $\vec{N}$ defined on M). Let $\Phi(t)$ be a smooth variation of immersions for $t \in (-\epsilon, \epsilon)$ so that $\Phi(0) = \Phi$ and $\Phi(t)|_{\partial M} = \Phi(0)|_{\partial M}$ for all $t \in (-\epsilon, \epsilon)$. Let $\vec{E}(t)$ be the variation vector field on $\Phi(t)$. We can assume, by reparametrizing $\Phi(t)$ for nonzero t if necessary, that the corresponding variation vector field at $t = 0$ is $\vec{E}(0) = u\vec{N}$, $u \in C_0^\infty(M)$. Let $a(t)$ be the area of $\Phi(t)(M)$ and H be the mean curvature of $\Phi(M)$. The first variational formula is

$$a'(0) := \frac{d}{dt} a(t) \Big|_{t=0} = -\int_M \langle nH\vec{N}, u\vec{N} \rangle dA,$$

where $\langle , \rangle$ and dA are the metric and area form on M induced by the immersion Φ. We now assume H is constant, so $a'(0) = -nH \int_M u \, dA$. Let $V(t)$ be the volume of $\Phi(t)(M)$, then $V'(0) = \int_M u \, dA$. The variation is *volume preserving* if

$\int_M \langle \vec{E}(t), \vec{N}(t) \rangle dA(t) = 0$ for all $t \in (-\epsilon, \epsilon)$. In particular, $\int_M u dA = 0$ when $t = 0$, so $a'(0) = 0$ and $\Phi(M)$ is critical for area amongst all volume preserving variations.

The second variation formula for volume preserving variations $\Phi(t)$ is

$$a''(0) := \frac{d^2}{dt^2} a(t) \bigg|_{t=0} = \int_M \{|\nabla u|^2 - (4H^2 - 2K)u^2\} dA = \int_M u L u dA \,,$$

where K is the Gaussian curvature on M induced by Φ, and

$$L = -\triangle - 4H^2 + 2K$$

is the Jacobi operator with Laplace-Beltrami operator $\triangle$.

There are two ways that the index of a smooth CMC surface can be defined:

The geometrically natural definition for index is the maximum possible dimension of a subspace $\mathcal{S}$ of volume preserving variation functions $u \in C_0^\infty(M)$ for which $a''(0) < 0$ for all nonzero $u \in \mathcal{S}$, which we call $\text{Ind}(M)$. (We are identifying $\Phi(M)$ with M so that we can write simply $\text{Ind}(M)$, rather than $\text{Ind}(\Phi(M))$.)

The analytically natural definition for index is the number of negative eigenvalues of the operator L, which equals the maximum possible dimension of a subspace $\mathcal{S}_U$ of (not necessarily volume preserving) variation functions $u \in C_0^\infty(M)$ for which $\int_M u L u dA < 0$ for all nonzero $u \in \mathcal{S}_U$. We call this index $\text{Ind}_U(M)$, where the subscript U stands for "Unconstrained index".

Clearly, $\text{Ind}_U(M) \geq \text{Ind}(M)$. It is also not difficult to see that $\text{Ind}_U(M) - 1 \leq \text{Ind}(M)$ [9]. As it is geometrically more natural, we want to compute $\text{Ind}(M)$. But $\text{Ind}_U(M)$ is more accessible to computation than $\text{Ind}(M)$, and since they differ by at most 1, computing $\text{Ind}_U(M)$ means that we know $\text{Ind}(M)$ is either $\text{Ind}_U(M)$ or $\text{Ind}_U(M) - 1$.

In the case that we are considering minimal surfaces, as in section 7, the volume constraint is not necessary, and hence $\text{Ind}(M) = \text{Ind}_U(M)$.

5.1. **Eigenvectors of L for Rectangles.** Consider the rectangle

$$M = \{(x, y, 0) \in \mathbb{R}^3 \,|\, 0 \leq x \leq x_0, 0 \leq y \leq y_0\}$$

as a smooth minimal immersion (inclusion map) into $\mathbb{R}^3$, and consider functions on it with Dirichlet boundary conditions. In this case, $L = -\triangle$, and its eigenvalues and eigenfunctions are

$$\lambda_{m,n} = \frac{m^2 \pi^2}{x_0^2} + \frac{n^2 \pi^2}{y_0^2} \,, \qquad \phi_{m,n} = \frac{2}{\sqrt{x_0 y_0}} \sin \frac{m \pi x}{x_0} \sin \frac{n \pi y}{y_0}$$

for $(m, n) \in \mathbb{Z}^+ \times \mathbb{Z}^+$. Hence $\text{Ind}(M) = 0$.

5.2. **Eigenvectors of L for Catenoids.** We can consider the catenoid as a map

$$\Phi : (x, y) \in \mathcal{R} \to (\cos x \cosh y, \sin x \cosh y, y) \in \mathbb{R}^3 \,,$$

where

$$\mathcal{R} = \{(x, y) \in \mathbb{R}^2 \,|\, 0 \leq x \leq 2\pi, y_0 \leq y \leq y_1\} \,,$$

and the left and right boundary segments of $\mathcal{R}$ are identified with each other. This is a conformal map, and the metric, Laplace-Beltrami operator, and Gauss curvature are

$$ds^2 = \cosh^2 y \cdot (dx^2 + dy^2) \,, \quad \triangle = \frac{\frac{\partial^2}{\partial^2 x} + \frac{\partial^2}{\partial^2 y}}{\cosh^2(y)} \,, \quad K = -\cosh^{-4} y \,.$$
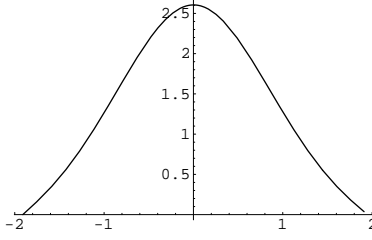
FIGURE 9. The function $f(y)$ (computed numerically) in the eigen-function $\cos(mx)f(y) = f(y)$ when $m = 0$ for the catenoid $\Phi(\mathcal{R})$ with $y_1 = -y_0 = 1.91$. The corresponding eigenvalue is $\lambda \approx -0.54$, and all other eigenvalues are positive. We show this function for later comparison with the first eigenvector field of the second variation of a discrete catenoid in section 7.

We put Dirichlet boundary conditions on the upper and lower boundary segments of $\mathcal{R}$.

Lemma 5.1. *An L^2-basis of eigenfunctions of the Jacobi operator $L = -\triangle + 2K$ of Φ can be chosen so the eigenfunctions are of the form $\sin(mx)f(y)$ or $\cos(mx)f(y)$, for $m \in \mathbb{N} \cup \{0\}$.*

Proof. It is well known that L, with respect to the Dirichlet boundary condition, has a discrete spectrum in $\mathbb{R}$, and that, for all $\lambda \in \mathbb{R}$, $\ker(L - \lambda)$ is a finite dimensional space of smooth functions. Furthermore, an orthonormal basis of the L^2 space over $\mathcal{R}$ (with respect to ds^2) can be obtained as a set of smooth eigenfunctions of L satisfying the Dirichlet boundary condition.

Define the operator $D = i\frac{\partial}{\partial x}$. Then $DL = LD$, so $D : \ker(L - \lambda) \to \ker(L - \lambda)$. For functions u and v that are 2π-periodic in x we have

$$\langle \frac{\partial}{\partial x}u, v\rangle_{L^2} + \langle u, \frac{\partial}{\partial x}v\rangle_{L^2} = \int_{\mathcal{R}} (u_x\overline{v} + u\overline{v}_x)\cosh^2 y\, dxdy = 0,$$

which implies that the operator $\frac{\partial}{\partial x}$ is skew symmetric. Therefore D is symmetric.

D is elliptic, so it has a basis of eigenfunctions in each finite dimensional space $\ker(L - \lambda)$. So we can choose a set of functions that is simultaneously an L^2-basis of eigenfunctions for both D and L. Since the eigenfunctions of D must be of the form $e^{mxi}f(y)$ with $m \in \mathbb{Z}$, the lemma follows. $\square$

Now note that an eigenfunction $\sin(mx)f(y)$ of L satisfies

$$\begin{aligned} L(\sin(mx)f(y)) &= \lambda\sin(mx)f(y) \\ &= \frac{m^2\sin(mx)f(y)}{\cosh^2 y} - \frac{\sin(mx)f_{yy}(y)}{\cosh^2 y} - \frac{2\sin(mx)f(y)}{\cosh^4 y}, \end{aligned}$$

and a similar computation holds for an eigenfunction $\cos(mx)f(y)$. It follows that

$$f_{yy} = (m^2 - \lambda\cosh^2 y - 2\cosh^{-2} y)f,$$

and finding the eigenvalues λ amounts to finding solutions of this equation that satisfy the boundary conditions $f(y_0) = f(y_1) = 0$. Thus we know all of the eigenfunctions, up to solutions of a determined 2nd-order ordinary differential equation.

6. Jacobi Operator for Discrete cmc Surfaces

Since we know the second variation matrix Q explicitly (section 4), we are now able to find the "discrete Jacobi operator" for compact discrete cmc surfaces $\mathcal{T}$, analogous to L in the smooth case (section 5). We first convert variation vector fields into piece-wise linear continuous functions, in order to naturally describe the L^2 norm on the space of variation vector fields. With this L^2 norm, we then find the correct matrix for the discrete Jacobi operator, and this matrix has the eigenvalues and eigenfunctions of the second variation of $\mathcal{T}$.

Consider a permissible variation

$$p_j(t) = p_j + t \cdot v_{p_j} + \mathcal{O}(t^2) \, ,$$

where the vector-valued function $v_{p_j} \in \mathbb{R}^3$ defined on the n interior vertices $\mathcal{V}_{int} = \{p_1, ..., p_n\}$ of $\mathcal{T}$ ($v_p = \vec{0}$ if p is a boundary vertex) comprises its variation vector field $\vec{v}^t = (v_{p_1}^t, ..., v_{p_n}^t)$, as defined in section 4.

There is a natural way to extend the function $\vec{v}$ to a continuous piece-wise linear $\mathbb{R}^3$-valued function v defined at every point of $\mathcal{T}$. In order to define v, we first define a set of piece-wise linear continuous head functions:

Definition 6.1. *For $p \in \mathcal{V}_{int}$, let ψ_p be the* head function *on $\mathcal{T}$ which is 1 at p and is 0 at all other vertices of $\mathcal{T}$. We then extend ψ_p to every point of $\mathcal{T}$ (in the unique way) so that it is linear on each edge and each face of $\mathcal{T}$.*

There is a head function for each $p_j \in \mathcal{V}_{int}$, hence there are n of them, and the support of ψ_{p_j} is $\text{star}(p_j)$.

Definition 6.2. *We define v associated to $\vec{v}$ by*

$$v|_T = v_p \psi_p + v_q \psi_q + v_r \psi_r,$$

for all triangles $T = (p, q, r)$ in $\mathcal{T}$.

The function v has the following four properties:

1. v is continuous,
2. v is linear on each triangle $T \subset \mathcal{T}$,
3. v is $\vec{0}$ on $\partial \mathcal{T}$,
4. v is the variation vector field for the C^0 surface variation induced by the associated vertex variation $p_j(t)$.

We will consider the v_{p_j} to be the $\mathbb{R}^3$-valued coefficients of v with respect to the basis of functions $\{\psi_{p_1}, ..., \psi_{p_n}\}$. And, as the ψ_{p_j} form a basis for all functions v with the above properties, they are a basis (with scalars in $\mathbb{R}^3$) for the following $3n$-dimensional function space:

Definition 6.3. *Define S_h of the discrete surface $\mathcal{T}$ to be*

$$S_h := \{v : \mathcal{T} \to \mathbb{R}^3 \,|\, v \in C^0(\mathcal{T}), \, v \text{ is linear on each } T \in \mathcal{T} \text{ and } v|_{\partial \mathcal{T}} = 0\} \, .$$

We have named this space S_h, in keeping with the notational conventions of the theory of finite elements. Note that the component functions of any function $v \in S_h$ all have bounded Sobolev H^1 norm.

Now we can find an explicit form for the L^2 inner product on S_h with respect to the basis $\{\psi_{p_1}, ..., \psi_{p_n}\}$:
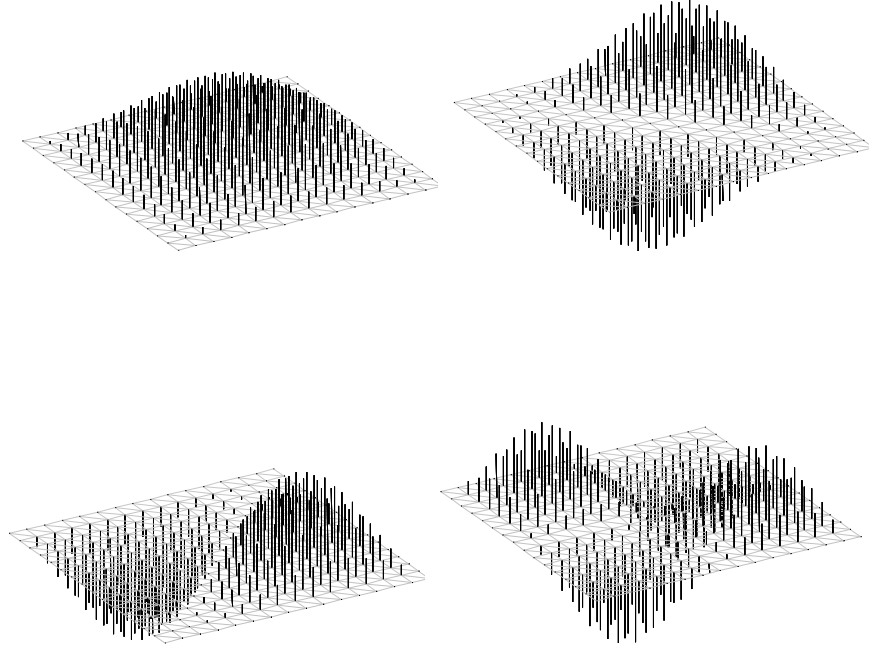
23

FIGURE 10. The eigenvectors of the discrete square with $n = 15$ associated to the eigenvalues λ_{392}, λ_{393}, λ_{394}, and λ_{395}. Note that these eigenvectors closely resemble the eigenfunctions $\sin(x)\sin(y)$, $\sin(x)\sin(2y) - \sin(2x)\sin(y)$, $\sin(x)\sin(2y) + \sin(2x)\sin(y)$, and $\sin(2x)\sin(2y)$ from the smooth case.

Proposition 6.1. *There is a positive definite $3n \times 3n$ matrix*

$$S = \left(\langle \psi_{p_i}, \psi_{p_j} \rangle_{L^2} I_{3 \times 3} \right)_{i,j=1}^{n}$$

so that

$$\langle u, v \rangle_{L^2} = \vec{u}^t S \vec{v}$$

for all $u, v \in S_h$ with associated vectors $\vec{u}, \vec{v} \in \mathbb{R}^{3n}$. The matrix S consists of 3×3 blocks $S_{p_i p_j}$ in an $n \times n$ grid, with the diagonal (resp. nondiagonal) blocks each being multiples of the 3×3 identity matrix,

$$S_{p_j p_j} = \left(\sum_{T \in \mathrm{star}(p_j)} \frac{|T|}{6} \right) I_{3 \times 3} , \quad resp. \quad S_{p_i p_j} = \left(\sum_{T \in \mathrm{star}(\overline{p_i p_j})} \frac{|T|}{12} \right) I_{3 \times 3}$$

when p_i and p_j are adjacent, and $S_{p_i p_j} = 0$ when p_i and p_j are not adjacent.

Proof. We first note that

$$|v|_{L^2}^2 := \int_{\mathcal{T}} \langle v, v \rangle dA = \sum_{T \subset \mathcal{T}} \int_T \langle v|_T, v|_T \rangle dA .$$

A computation yields that for each triangle $T \subset \mathcal{T}$,

$$\int_T \psi_p^2 dA = \frac{|T|}{6} , \quad \int_T \psi_p \psi_q dA = \frac{|T|}{12} ,$$
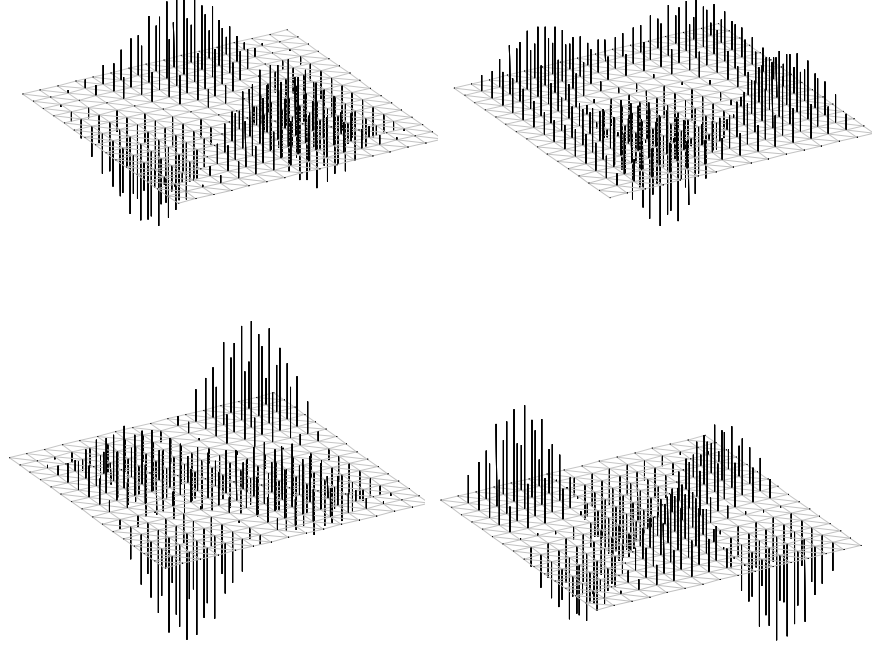
FIGURE 11. The eigenvectors of the discrete square with $n = 15$ associated to the eigenvalues λ_{396}, λ_{397}, λ_{398}, and λ_{399}. Note that these eigenvectors closely resemble the eigenfunctions $\sin(3x)\sin(y) - \sin(x)\sin(3y)$, $\sin(3x)\sin(y) + \sin(x)\sin(3y)$, $\sin(3x)\sin(2y) - \sin(2x)\sin(3y)$, and $-\sin(3x)\sin(2y) - \sin(2x)\sin(3y)$ from the smooth case.

for any vertices p and q of T. Thus

$$|v|_{L^2}^2 = \sum_{T=(p,q,r)\in\mathcal{T}} \frac{|T|}{6}\{|v_p|^2 + |v_q|^2 + |v_r|^2 + \langle v_p, v_q \rangle + \langle v_p, v_r \rangle + \langle v_q, v_r \rangle\} \ .$$

Hence, for any two functions $u, v \in S_h$, we have

$$\langle u, v \rangle_{L^2} =$$

$$\sum_{T=(p,q,r)\in\mathcal{T}} \frac{|T|}{12}\{\langle u_p + u_q + u_r, v_p + v_q + v_r \rangle + \langle u_p, v_p \rangle + \langle u_q, v_q \rangle + \langle u_r, v_r \rangle\}$$

$$= \sum_{p_j \in \mathcal{V}_{int}} \left(\langle u_{p_j}, v_{p_j} \rangle \left(\sum_{T \in \text{star}(p_j)} \frac{|T|}{6} \right) + \right.$$

$$\left. \sum_{p_i \in \mathcal{V}_{int} \text{ adjacent to } p_j} \langle u_{p_j}, v_{p_i} \rangle \left(\sum_{T \in \text{star}(\overline{p_i p_j})} \frac{|T|}{12} \right) \right) \ .$$

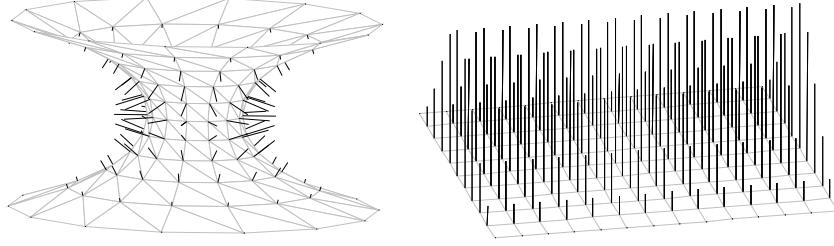Hence the 3×3 blocks $S_{p_i p_j}$ are as in the proposition. $\qquad \square$

FIGURE 12. The eigenvector associated to the eigenvalue $\lambda_0 \approx -0.542$ of a discrete catenoid. Here we have also shown this $\mathbb{R}^{3n}$-vector field on a horizontal planar grid (where each $\mathbb{R}^3$-vector is vertical with length equal to that of the corresponding $\mathbb{R}^3$-vector in the $\mathbb{R}^{3n}$-eigenvector field on the discrete catenoid), so that we can compare it directly with the eigenfunction shown in Figure 9 for the smooth case. Notice that the plot on the right closely resembles the curve in Figure 9.

We now compute the discrete Jacobi operator $L_h : S_h \to S_h$ associated to the second variation formula for the surface, i.e. $\int_{\mathcal{T}} v^t L_h v \, dA = \vec{v}^{\,t} Q \vec{v}$ for all $v \in S_h$ (recall that $Q = Q_a - H Q_V$). We need the property $L_h(S_h) \subset S_h$ so that we can consider the eigenvalue problem for L_h. And we also wish L_h to be linear and symmetric ($\int_{\mathcal{T}} u^t L_h v = \int_{\mathcal{T}} v^t L_h u$ for all $u, v \in S_h$). With these properties, the choice of L_h is canonical:

Proposition 6.2. *There exists a unique linear operator $L_h : S_h \to S_h$ so that $\int_{\mathcal{T}} u^t L_h v \, dA$ is symmetric in u and v and*

$$\int_{\mathcal{T}} v^t L_h v \, dA = \vec{v}^{\,t} Q \vec{v}$$

for all $v \in S_h$. Furthermore, if v is the function in S_h associated to the $\mathbb{R}^{3n}$-vector $\vec{v}$, then $L_h v$ is the function in S_h associated to the $\mathbb{R}^{3n}$-vector

$$S^{-1} Q \vec{v} \,.$$

Proof. For $v = \sum_{j=1}^{n} v_{p_j} \psi_{p_j}$, we define

$$L_h v := \sum_{i,j,k=1}^{n} (S^{-1})_{p_i p_k} ((Q_{a, p_k p_j} - H Q_{V, p_k p_j}) v_{p_j}) \psi_{p_i} \,,$$

which is the function in S_h associated to $S^{-1} Q \vec{v}$. This map L_h is clearly linear, and

$$\int_{\mathcal{T}} u^t L_h v \, dA = \langle u, L_h v \rangle_{L^2} = \vec{u} S (S^{-1} Q \vec{v}) = \vec{u}^{\,t} Q \vec{v}$$

for all $u, v \in S_h$. Hence, since Q is symmetric, $\int_{\mathcal{T}} u^t L_h v \, dA$ is symmetric in u and v.

Uniqueness of L_h with the above properties follows from the following:

$$\int_{\mathcal{T}} u^t L_h v \, dA = \frac{1}{2} \left(\int_{\mathcal{T}} (u+v)^t L_h (u+v) \, dA - \int_{\mathcal{T}} u^t L_h u \, dA - \int_{\mathcal{T}} v^t L_h v \, dA \right)$$
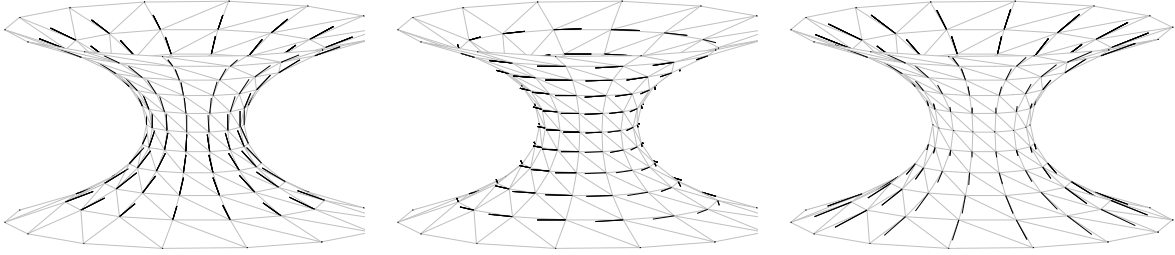
FIGURE 13. Two-thirds of the eigenvectors are approximately tangential to the surface. For example, here we show the $\mathbb{R}^{3n}$-eigenvector fields associated to the eigenvalues λ_1, λ_2, and λ_3 (whose values are just slightly greater than 0).

$$= \frac{1}{2} \left((\vec{u} + \vec{v})^t Q (\vec{u} + \vec{v}) - \vec{u}^t Q \vec{u} - \vec{v}^t Q \vec{v} \right) .$$

Hence $\int_{\mathcal{T}} u^t L_h v \, dA$ is uniquely determined for all $u \in S_h$, so $L_h v$ is uniquely determined for each $v \in S_h$. □

So the spectrum of the second variation of $\mathcal{T}$ is the set of eigenvalues of $S^{-1}Q$. One can check that $S^{-1}Q$ is self-adjoint with respect to the L^2 inner product on S_h, thus all the eigenvalues of $S^{-1}Q$ are real.

Remark 6.1. *Another way to see that $S^{-1}Q$ is the correct discrete Jacobi operator is to consider the Rayleigh quotient*

$$\frac{\vec{v}^t Q \vec{v}}{\langle v, v \rangle_{L^2}} = \frac{\vec{v}^t S (S^{-1} Q \vec{v})}{\vec{v}^t S \vec{v}} .$$

Using the standard procedure for producing eigenvalues from the Rayleigh quotient in this case would produce the eigenvalues of $S^{-1}Q$.

7. APPROXIMATING SPECTRA OF SMOOTH CMC SURFACES

We can now implement the procedure described in the second half of the introduction, since we know $S^{-1}Q$ explicitly.

If a sequence of compact CMC discrete surfaces $\{\mathcal{T}\}_{i=1}^{\infty}$ converges (in the Sobolev H^1 norm as graphs over the limiting surface) to a smooth compact CMC surface $\Phi : M \to \mathbb{R}^3$, then standard estimates from the theory of finite elements (see, for example, [3] or [7]) imply that the eigenvalues and eigenvectors (piece-wise linearly extended to functions) of the operators L_h of the $\mathcal{T}_j$ converge to the eigenvalues and eigenfunctions of the Jacobi operator L of Φ (convergence is in the L^2 norm for the eigenfunctions).

For the first two examples here – a planar square and rotationally symmetric portion of a catenoid – we know the approximating discrete minimal surfaces exactly, and we know the eigenvalues and eigenfunctions of L for the smooth minimal surfaces exactly, so we can check that convergence of the eigenvalues and eigenfunctions does indeed occur.

In the final example – a symmetric portion of a trinoid – the spectrum of the smooth minimal surface is unknown, so we see estimates for the eigenvalues and eigenfunctions for the first time. Our experiments confirm the known value 3 for the index of this unstable surface, and additionally show us the directions of variations
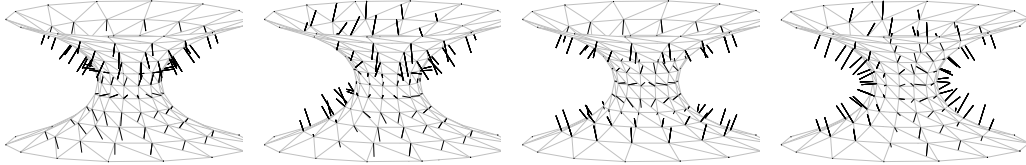
FIGURE 14. One-third of the eigenvectors are approximately perpendicular to the surface. For example, here we show the $\mathbb{R}^{3n}$-eigenvector fields associated to the eigenvalues λ_{147}, λ_{171}, λ_{204}, and λ_{210}.

that reduce area. Thus we have approximations for maximal spaces of variation vector fields on the smooth minimal surfaces for which the associated variations reduce area. (For the approximating discrete surfaces in this example, we do not have an explicit form; however, the theory of finite elements applies and we can still expect convergence of the eigenvalues and eigenfunctions (in L^2 norm), if we choose the discrete aproximations so that they converge (in H^1 norm) to the smooth minimal surfaces.)

7.1. **The flat minimal square.** Considering the square $M = \{0 \le x \le \pi, 0 \le y \le \pi\}$ included in $\mathbb{R}^3$ as a smooth minimal surface, the eigenvalues and eigenfunctions of L are $\mu_{m,n} = m^2 + n^2$ and $\phi_{m,n} = \frac{2}{\pi}\sin(mx)\sin(ny)$ for $m, n \in \mathbb{Z}^+$ (section 5).

Now we consider the discrete minimal surface $\mathcal{T}$ that is M with a regular square $n \times n$ grid. In each subsquare of dimension $\frac{\pi}{n} \times \frac{\pi}{n}$, we draw an edge from the lower left corner to the upper right corner, producing a discrete minimal surface with $2n^2$ congruent triangles with angles $\frac{\pi}{4}$, $\frac{\pi}{4}$, and $\frac{\pi}{2}$.

For this $\mathcal{T}$, $S^{-1}Q$ has no negative eigenvalues, as expected, since the smooth minimal square is stable. However, we must take tangential motions into account in the discrete case, and we find that (when writing the eigenvalues in increasing order) the first two-thirds of the eigenvalues are 0 and their associated eigenvectors are entirely tangent to the surface. The final one-third of the eigenvalues are positive, with eigenvectors that are exactly perpendicular to the surface. Examples of these perpendicular vector fields are shown in Figures 10 and 11 for $n = 15$. (There are 196 interior vertices, and so there are 588 eigenvalues λ_j of $S^{-1}Q$ and $\lambda_0 = ... = \lambda_{391} = 0$ and $\lambda_j > 0$ when $j \in [392, 587]$.) The eigenvectors shown in these figures and their eigenvalues are close to those of the smooth operator L of M. We have $\lambda_{392} = 2.022 \approx \mu_{1,1}$, $\lambda_{393} = 5.094 \approx \mu_{1,2}$, $\lambda_{394} = 5.148 \approx \mu_{2,1}$, $\lambda_{395} = 8.347 \approx \mu_{2,2}$, $\lambda_{396} = 10.434 \approx \mu_{1,3}$, $\lambda_{397} = 10.445 \approx \mu_{3,1}$, $\lambda_{398} = 13.649 \approx \mu_{2,3}$, $\lambda_{399} = 14.12 \approx \mu_{3,2}$.

7.2. **Discrete Minimal Catenoids.** By Corollary 3.2, we know that the discrete minimal catenoids converge to smooth catenoids as the meshes are made finer. Hence the eigenvalues and eigenvectors of the discrete catenoids converge to the eigenvalues and eigenfunctions of the smooth catenoid. For the discrete catenoids with relatively fine meshes, we find that two-thirds of the eigenvectors are approximately tangent to the surface, and the remaining ones are approximately perpendicular. The approximately perpendicular ones (considered as functions which are multiplied by unit normal vectors) and their eigenvalues converge to the eigenfunctions and eigenvalues of the smooth catenoid (computed in section 5).
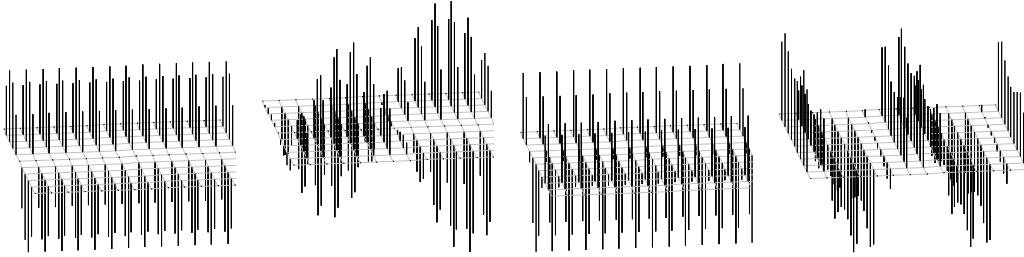
FIGURE 15. Here we show the projected versions of the eigenvectors in the previous figure, for use in comparing with the eigenfunctions of the smooth case considered in section 5. These projected versions are made the same way as in Figure 12.

Consider the example shown in the Figures 12, 13, 14, and 15. Here the catenoid has $9 \times 14 = 126$ interior vertices, so the matrix $S^{-1}Q$ has dimension 378×378. The first eigenvalue of this matrix is $\lambda_0 \approx -0.542$ and $\lambda_j > 0$ for all $j \in [1, 377]$, as expected, since the smooth complete catenoid has index 1 ([6]). Note that λ_0 is very close to the negative eigenvalue for the smooth case, described in the caption of Figure 9 (the closest matching smooth catenoid portion satisfies $y_1 = -y_0 = 1.91$). The first eigenfunction in the discrete case (Figure 12) is also very close to the first eigenfunction in the smooth case (Figure 9).

7.3. **Discrete Minimal Trinoids.** Since the trinoid has index 3, we find that approximating discrete surfaces with relatively fine meshes have 3 negative eigenvalues. And we can look at the corresponding eigenvector fields (which estimate the eigenfunctions in the smooth case), shown in Figure 16. For the approximating discrete trinoid in Figure 16, the first four eigenvalues are approximately $-3.79, -1.31, -1.31, 0.014$, so we indeed have 3 negative eigenvalues and the second eigenvalue has multiplicity 2.

REFERENCES

[1] J. L. Barbosa and M. do Carmo. Stability of minimal surfaces and eigenvalues of the laplacian. *Math. Z.*, 173:13–28, 1980.

[2] A. Bobenko and U. Pinkall. Discrete isothermic surfaces. *J. reine angew. Math.*, 475:187–208, 1996.

[3] S. C. Brenner and L. R. Scott. The mathematical theory of finite element methods. Springer-Verlag, 1994.

[4] D. Bressoud and J. Propp. How the alternating sign matrix conjecture was solved. *Notices of the AMS*, 46(6):637–646, 1999.

[5] J. Dodziuk and V. K. Patodi. Riemannian structures and triangulations of manifolds. *J. Indian Math Soc* 40:1-52, 1976.

[6] D. Fischer-Colbrie. On complete minimal surfaces with finite Morse index in three manifolds. *Invent. Math.* 82:121-132, 1985.

[7] G. Fix and G. Strang. An analysis of the finite element method. Prentice-Hall, 1973.

[8] M. Gromov. Metric structures for Riemannian and non-Riemannian spaces. Progress in Mathematics, vol. 152, Springer-Verlag, 1999.

[9] L.L. de Lima and W. Rossman. On the index of constant mean curvature 1 surfaces in hyperbolic space *Indiana Math. J.* 47(2):685-723, 1998.

[10] S. Montiel and A. Ros. Schrödinger operators associated to a holomorphic map. Global Differential Geometry and Global Analysis, Lect. Notes in Math. # 1481, Berlin 1991, 147-174.
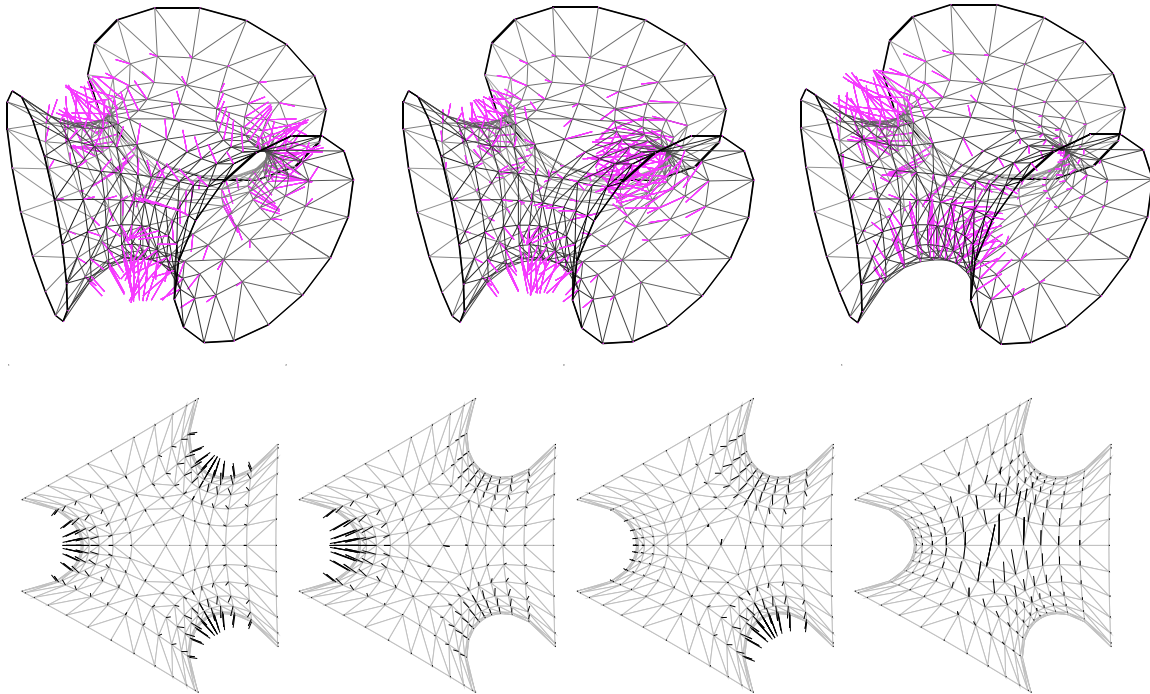
FIGURE 16. Variation vector fields for three area-reducing variations of a discrete approximation of a compact portion of a trinoid. The lower row has overhead views of these variation vector fields, as well as an overhead view of the variation vector field associated to the fourth (and first positive) eigenvalue.
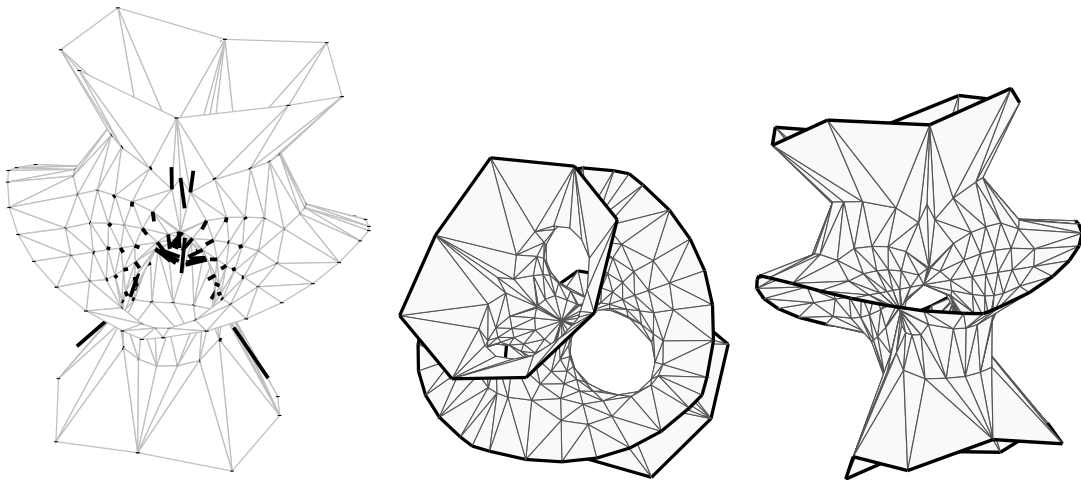

FIGURE 17. The first eigenvector field (whose corresponding eigenvalue is the first one and is negative) for a discrete approximation of a compact portion of a genus 1 Costa surface. Two other views of this discrete surface are shown.
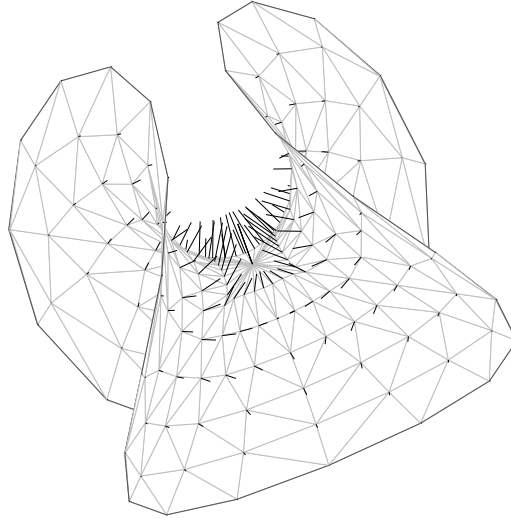
FIGURE 18. The first eigenvector field for a discrete approximation of a compact portion of an Enneper surface. The associated first eigenvalue is negative and is the only negative eigenvalue that is not approximately zero, corresponding to the fact that the smooth Enneper surface has index 1. Those other negative (approximately zero) eigenvalues have corresponding eigenvector fields that appear roughly tangent to the surface.

[11] S. Nayatani. Lower bounds for the morse index of complete minimal surfaces in Euclidean 3-space. *Osaka J. Math.*, 27:453-464, 1990.
[12] S. Nayatani. Morse index of complete minimal surfaces. *The Problem of Plateau*, ed. by Th. M. Rassias, World Scientific (1992), 181-189.
[13] S. Nayatani. Morse index and Gauss maps of complete minimal surfaces in Euclidean 3-space. *Comment. Math. Helv.* 68:511-537, 1993.
[14] B. Oberknapp and K. Polthier. An algorithm for discrete constant mean curvature surfaces. In H.-C. Hege and K. Polthier, editors, *Visualization and Mathematics*, pages 141–161. Springer Verlag, Heidelberg, 1997.
[15] R. Osserman. *A Survey of Minimal Surfaces*. Dover, 1986.
[16] U. Pinkall and K. Polthier. Computing discrete minimal surfaces and their conjugates. *Experim. Math.*, 2(1):15–36, 1993.
[17] K. Polthier. Conjugate harmonic maps and minimal surfaces. *preprint*, 2000.